energy&fuels

pubs.acs.org/EF
Article

Sustainable Bioproducts of Coconut Husk Biomass—Part I: Pyrolytic Conversion into Biochar, Bio-Oil, and Pyrolytic Gas

Published as part of Energy & Fuels special issue "PyroLiq 2025".

Tarcísio Martins, Mirele Santana Sá, Miliana Gouveia Silva, Wenes Ramos da Silva, and Alberto Wisniewski, Jr.*

Cite This: https://doi.org/10.1021/acs.energyfuels.5c06504

ABSTRACT: Given the large amount of green coconut husk (GCH) waste generated in Brazil and the environmental impacts of improper disposal, this study evaluated pyrolysis as a method for managing and adding value to residual GCH biomass by producing value-added products. GCH exhibited properties suitable for pyrolysis, including high volatile content, low ash content, and a higher heating value (HHV) of approximately 22 MJ kg^{-1}. Pyrolysis was carried out in a rotary kiln reactor operated at 400, 500, and 600 °C, yielding biochars (29−47 wt %) and bio-oils (6.6−11 wt %). Increasing the temperature intensified biomass thermal degradation, resulting in higher gas production (up to 31.4 wt %). The 400 °C biochar had a higher yield and greater organic functionalization, making it suitable as an adsorbent; the 600 °C biochar had a more aromatic and stable structure, making it promising for carbon sequestration; and the 500 °C biochar balanced functionalization and stability, broadening its application potential. The bio-oils had calorific values between 26 and 31 MJ kg^{-1} and moderate viscosity. The highest yield (∼11 wt %) and phenolic monomer content (∼50% by area) were obtained at 500 °C, highlighting the product's potential for industrial use. The results indicate that pyrolysis at 500 °C is the most favorable condition for the energy and chemical utilization of green coconut biomass, providing a sustainable and viable route for producing value-added bioproducts.

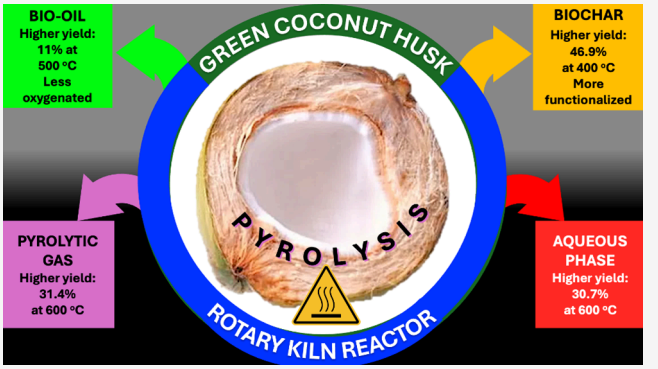

1. INTRODUCTION

The rising demand for energy and raw materials, along with increasing environmental concerns, has driven the search for more sustainable alternatives in the energy and industrial sectors.[1] In this context, the use of abundant and carbon-neutral raw materials, such as lignocellulosic biomass, stands out as one of the most promising renewable sources for large-scale production of sustainable chemical inputs and materials with potential value in the carbon credit market.[2] In addition to providing renewable resources for energy and industrial applications, converting lignocellulosic biomass is also an efficient strategy for managing urban and agricultural waste, which is traditionally considered an environmental liability, such as green coconut husks (GCH).[3]

According to data from the Food and Agriculture Organization (FAO) and the Brazilian Institute of Geography and Statistics (IBGE), Brazil produces an average of approximately 2.8 million tons of coconut per year, which corresponds to around 1.9 billion fruits.[4,5] Brazilian production is mainly concentrated in the northeast region, especially along the coast, which accounts for about 80% of the country's total. Located in the Brazilian Northeast, the state of Sergipe is the sixth largest coconut producer in the country, with an average annual production of 131.6 million fruits.

The main market for this fruit in Brazil is the commercialization of coconut water, which creates a high demand for immature fruits.[6] After coconut water is extracted, it is estimated that about 80% of the fruit's mass remains as GCH residue.[7,8] Based on these data, it is estimated that the Brazilian coconut processing chain generates around 2 million tons of husk per year, while in the state of Sergipe this volume is approximately 140,000 tons per year (wet basis). Due to challenges involved in managing it, this material is often sent to landfills and dumps, contributing to the accumulation of solid waste, the emission of polluting gases from decomposition, the

Received: December 11, 2025
Revised: February 25, 2026
Accepted: February 26, 2026
Published: March 10, 2026

proliferation of parasites, and the contamination of soil and groundwater.[9] As a lignocellulosic waste produced in large quantities and with potential as a biomass source, there is a growing interest in exploring processing technologies capable of handling large amounts of GCH waste, as well as being efficient in recovering the value of the raw material.

Considering research on the valorization of waste biomass, the application of thermochemical technologies can diversify the range of products obtained, including renewable-based chemical inputs for the industrial and energy sectors, agricultural supplements and technologies for carbon sequestration.[10,11] Among the thermochemical processes used to valorize lignocellulosic waste, pyrolysis is identified as one of the technologies with the greatest potential for industrial growth, with technological readiness levels ranging from 6 to 9.[12] Among the products obtained from the pyrolysis of lignocellulosic waste, biochar and bio-oil are notable for their wide range of applications, spanning the agricultural, industrial, and energy sectors.

Biochar is a carbonaceous material rich in organic functional groups, with a high fixed carbon content and has a porous structure with a high surface area.[13] Some studies reported applications for GCH-biochar as an electrocatalyst for CO_2 reduction,[14] an adsorbent emerging pollutants removal,[15] and in agricultural applications.[16] About bio-oil, this product consists of a mixture of organic compounds that can be applied in various sectors of the economy, which can be converted into biofuel or employed as a feedstock for the chemical industry, reducing the demand for crude oil derivatives.[17] Studies that evaluated the production of bio-oil from GCH wastes reported a high abundance of phenolic compounds, attributed to the high lignin content present in the biomass.[18,19]

It is important to highlight that the yield and properties of pyrolysis products are influenced by both the characteristics of the biomass and the operating conditions of the process, which can be optimized for specific applications.[20] As pyrolysis is an endothermic process, temperature is one of the most critical operating parameters, significantly affecting the conversion rate of the raw material and the physical and chemical properties of the resulting products.[21] For this reason, the operating temperature of the pyrolysis reactor is the main variable evaluated in process optimization studies for converting lignocellulosic waste into biochar, bio-oil and gases.[21−24]

Few studies have investigated the effect of temperature on the pyrolysis of GCH residues. Most of the available research focuses primarily on how this parameter influences the characteristics of biochar and its potential applications.[16,25,26] The most comprehensive study addressing the influence of temperature on GCH biochar properties is that of Dhar et al.,[27] who examined the physicochemical properties of biochar produced from the slow pyrolysis of green coconut fibers at different temperatures. The authors reported that increasing the pyrolysis temperature reduced biochar yield but improved key properties such as carbon content, alkalinity, and surface area, thereby enhancing its suitability for agricultural applications. In contrast, studies on bio-oil are still scarce. There are no representative investigations evaluating how pyrolysis temperature affects the chemical composition of bio-oil derived from GCH residues.

In this context, given the significant amount of green coconut waste generated during commercialization, the environmental impacts of improper disposal, and especially its potential as a lignocellulosic feedstock for producing value-added renewable inputs, this study investigated the valorization of residual green coconut husk biomass through pyrolysis, with emphasis on in-depth chemical characterization of products obtained at different temperatures (400, 500, and 600 °C), especially for bio-oil, which is underexplored in the literature for this biomass. The yields and chemical compositions of the products derived from the pyrolysis of GCH waste were analyzed to assess the effect of pyrolysis temperature on their chemical characteristics and potential applications, highlighting the role of pyrolysis as a strategy for managing and adding value to residual biomass from the coconut processing chain. This work provides a comprehensive basis on the influence of pyrolysis temperature on the characteristics of all products obtained from the pyrolysis of GCH, an approach not yet explored in an integrated way in the literature.

2. MATERIALS AND METHODS

2.1. Biomass Preparation

The GCH waste was collected from a local coconut water retailer in São Cristóvão, Sergipe, Brazil. Initially, the raw husks were ground in a knife and hammer mill to unpack the fruit. The in natura moisture content of the material collected was determined in an oven at 105 °C for 24 h and found to be 76.5% ± 1.2%. To reduce this parameter to below 10%, the collected material was sun-dried for 15 days. After this period, the biomass was ground again to obtain a particle size ≤2 mm. Finally, the dried and crushed material was stored and subjected to physical and chemical analysis, as well as pyrolysis experiments.

2.2. Feedstock Characterization

2.2.1. Proximate and Elemental Analysis. The proximate analysis of the GCH biomass to determine the moisture, volatile material, fixed carbon and ash contents was carried out in accordance with ASTM D1762-84 (2013), using approximately 1.0 g of biomass. About the elemental composition of GCH wastes, the carbon (C), hydrogen (H) and nitrogen (N) contents were determined using a LECO CHN628 instrument (LECO Corporation, St. Joseph, MI, USA), based on the analysis of 50 mg of biomass packed in tin foil and quantified using an EDTA analytical curve (10−200 mg). The oxygen (O) content was estimated by difference, considering the ash content obtained during the proximate analysis. Based on this data, the biomass' higher heating value (HHV) was calculated using the model developed by Huang et al.[28]

2.2.2. Vegetable Oil Content and Fatty Acids Composition. The vegetable oil content of GCH was determined by ultrasound-assisted *n*-hexane extraction, using around 2 g of biomass and 20 mL of solvent in a round- bottom flask, with ultrasonication for 1 h. After filtration and evaporation of the solvent, the oil was quantified based on mass difference. The extracted material was then subjected to transesterification to convert the triacylglycerols into methyl esters whose fatty acid composition was determined by gas chromatography−mass spectrometry (GC−MS), following a standard laboratory protocol.

The fatty acids methyl esters were prepared as follows: ∼25 mg of the extract was mixed with 2 mL of a NaOH methanolic solution at 2% (m/v). The mixture was heated at 40 °C under constant stirring for 5 min. Then 3 mL of a 5% (m/m) H_2SO_4 solution, prepared in a 3% (m/v) NH_4Cl methanolic solution, was added. The mixture was heated again to 40 °C and kept under constant stirring for a further 3 min. Subsequently, 2.5 mL of a saturated aqueous $NaHCO_3$ solution was added for neutralization. The organic phase was then extracted with 2.5 mL of *n*-hexane, diluted four times using the same solvent and subjected to chromatographic analysis using a gas chromatograph (model TRACE 1310, Thermo Scientific, Bremen, Germany) coupled to a mass spectrometer (model TSQ-9000, Thermo Scientific, Bremen, Germany), under the analytical conditions described by Melo et al.[29]

https://doi.org/10.1021/acs.energyfuels.5c06504
Energy Fuels XXXX, XXX, XXX−XXX

2.2.3. Thermogravimetric Analysis (TGA) and Lignocellulosic Composition Estimation. The thermogravimetric behavior of GCH was determined using a Shimadzu TGA-50 thermogravimetric analyzer with a sensitivity of 0.001 mg. The equipment was operated using a 75 μL platinum crucible in a nitrogen (N_2) flow rate of 50 mL min^{-1}. Approximately 8 mg of biomass was heated from 30 to 800 °C at a heating rate of 10 °C min^{-1}, while the mass loss was continuously monitored, to obtain thermogravimetric curves (TGA) and their derivative (DTG).

From the TGA and DTG curves, it was possible to estimate the lignocellulosic composition of GCH waste. Initially, the DTG curve was subjected to a deconvolution process using Gaussian multiple peak fitting. In this process, the DTG curve was modeled with five main regions corresponding to mass losses from moisture evaporation, release of extractables, and thermal degradation of hemicellulose, cellulose, and lignin. The nonlinear adjustments were performed using the Levenberg−Marquardt algorithm, and the deconvolution process yielded a coefficient of determination (R^2) of 0.995. Once obtained, the curves of the individual biomass components were integrated and from this it was possible to estimate the lignocellulosic composition of GCH using the procedure described in Moura et al.[30]

2.3. Biomass Pyrolysis Experiments

The experiments were carried out continuously in a semipilot scale reactor with a rotary kiln (Adapted from Model FRO 1100, ForteLab Ltd.a, Brazil). The diagram of the reactor used is shown in the Supporting Information (Figure S1). The biomass was processed at three temperatures (400, 500, and 600 °C), while the other operating conditions were maintained as follows: dry biomass mass of ∼0.5 kg (feed at ∼0.75 kg h^{-1}), feeder rotation at 6 rpm, feeder vibration intensity at 90 arbitrary units, kiln inclination at 15°, cylinder rotation at 7.5 rpm, continuous N_2 flow at 5 L min^{-1} and total pyrolysis time of around 40 min.

The biochar produced was continuously collected in the solid's reception container at the reactor outlet. The pyrolytic vapors were drawn in by a low-vacuum pump and directed to a condensation system with three condensers arranged in series, each with recirculating water at 5 °C. The pyrolysis liquids were collected in a two-way flask. After collecting the liquid product, the noncondensable fraction was sent to a gas washing system to remove light volatiles from the gas phase. The washing system consisting of three tanks arranged in series containing, respectively: (1) 1 mol L^{-1} NaOH solution, (2) 1 mol L^{-1} Na_2SO_3 solution, and (3) 1 mol L^{-1} CH_3COOH solution. This was then discarded, as shown in Figure S1.

A sampling point for the gaseous product was installed between the condensation system and the gas washing system. Samples were collected using a gastight syringe and stored in appropriate sampling bags. Before the experiment began, a blank reference sample containing only N_2 was collected. Pyrolysis time was measured from the moment the biomass was fed into the reactor and gases exited the system. After timing began, samples of the pyrolysis gases were taken at 5 min intervals throughout the process, totaling six samples between 5 and 30 min of the experiment.

At the end of the experiment, the collected products were weighed. After dismantling the system, some coke remained adhered to the walls of the cyclone at the reactor outlet; this fraction was also collected and weighed. Product yields were calculated based on the mass of raw material fed into the reactor. To estimate the amount of organic material in the aqueous pyrolysis fraction, approximately 10 mL of the product was freeze-dried. The mass of the resulting dry organic material was measured and expressed as a mass/volume percentage (m/v %).

2.4. Pyrolytic Products Characterization

2.4.1. Physical-Chemical Characterization. The biochars were characterized by proximate analysis using the protocol described in ASTM D1762-84 (2013). The presence of acidic or basic functional groups in the carbonaceous materials was assessed by determining the pH of aqueous solutions containing the biochars, prepared by mixing 1 g of the material in 25 mL of deionized water, followed by stirring for 1 h and then resting for 30 min. The pH was measured using a PHOX pH meter, model P1000. All procedures were performed in triplicate. For elemental composition, the biochars and bio-oils were analyzed following the methodology described in section 2.2.1. For the bio-oil, approximately 50 mg of sample was added on a tin foil using Aid for Liquids (LECO Corp.). Bio-oil's water content was determined by Karl Fischer titration, using ∼20−50 mg of the raw samples. The distribution of inorganic elements in the biochar samples was determined by Energy-Dispersive X-ray Fluorescence Spectroscopy on a Shimadzu instrument, model EDX-720/800HS, with a range covering Na to Sc atoms (15 kV) and Ti to U atoms (50 kV), using the automatic screening method.

2.4.2. Fourier-Transform Infrared Spectroscopy (FTIR). The functional groups present in the biochars and bio-oils were identified by FTIR analysis using a PerkinElmer Spectrum Two spectrophotometer (PerkinElmer, USA), operating with a spectral range of 4000 to 400 cm^{-1}, a resolution of 4 cm^{-1} and an acquisition rate of 32 scans/min. The samples were prepared by maceration with KBr (in a ratio of 1 mg of sample to 100 mg of KBr), pressed to form pellets and then submitted to spectroscopic analysis.

2.4.3. Pyrolytic Gases Characterization by GC-TCD. The samples collected during the pyrolysis process were analyzed using an Agilent 490 Micro-GC gas chromatograph (Agilent Technologies, Santa Clara, CA, USA) equipped with a thermal conductivity detector (TCD). The system has a module with two channels: the first channel contains a CP-Molsieve 5A column and operates with argon as the carrier gas; the second channel is equipped with a CP-PoraPLOT U column and uses helium as the carrier gas. Both chromatographic columns are 10 m long. The constituents of the pyrolysis gas were quantified using an analytical curve constructed with a standard mixture composed of hydrogen (H_2), nitrogen (N_2), methane (CH_4), carbon monoxide (CO), carbon dioxide (CO_2), ethane (C_2H_6), ethylene (C_2H_4), acetylene (C_2H_2), and propane (C_3H_8). The operating conditions were as follows: injector temperature of 50 °C with an injection time of 50 ms; initial pressures of 25 and 20 psi in the first and second channels, respectively; furnace temperatures of 70 and 50 °C in the first and second channels, respectively.

The analysis results were expressed as the molar composition (mol/mol %) of the gas mixture produced during the pyrolysis process. As a parameter for assessing the reaction stability of the process, the composition of the pyrolytic gas was monitored throughout the experiment (0 to 30 min). To quantify the gaseous species, the average composition of the pyrolysis gas was used to calculate the molar mass of the mixture, using the molar masses of the individual components weighted by their respective fractions, according to eq 1, where, y_i is the molar fraction of component "i" in the mixture and M_i is its molar mass (g mol^{-1}).

$$M_{\text{Pyrolyticgas}} = \sum y_i M_i \ [\text{g mol}^{-1}] \tag{1}$$

After determining the average molar mass of the mixture, the number of moles of the gaseous product was calculated according to the eq 2, where Y_{gas} corresponds to the yield of gaseous product during pyrolysis and m_{GCH} is the mass of biomass used in the experiment.

$$n_{\text{Pyrolyticgas}} = \frac{(Y_{\text{gas}} \times m_{\text{GCH}})}{M_{\text{Pyrolyticgas}}} \ [\text{mol}] \tag{2}$$

Subsequently, the volume of each gas species was determined using the ideal gas law ($PV = nRT$), relating this volume to the mass of biomass used in the pyrolysis. This allowed calculation of the conversion (L/kg_{GCH}), according to eq 3.

$$\text{Conversion}_i(v_i/m_{\text{GCH}}) = \left[\frac{(y_i \times n_{\text{Pyrolyticgas}}) \times R \times T\ (298\ \text{K})}{P\ (1\text{atm})}\right] \times \left(\frac{1000}{m_{\text{GCH}}}\right)\left[\frac{\text{L}}{\text{kg}_{\text{GCH}}}\right] \tag{3}$$

Where y_i is the mole fraction of component "i" in the mixture, $n_{\text{Pyrolyticgas}}$ is the number of moles of pyrolysis gas (eq 2), R is the

https://doi.org/10.1021/acs.energyfuels.5c06504
Energy Fuels XXXX, XXX, XXX−XXX

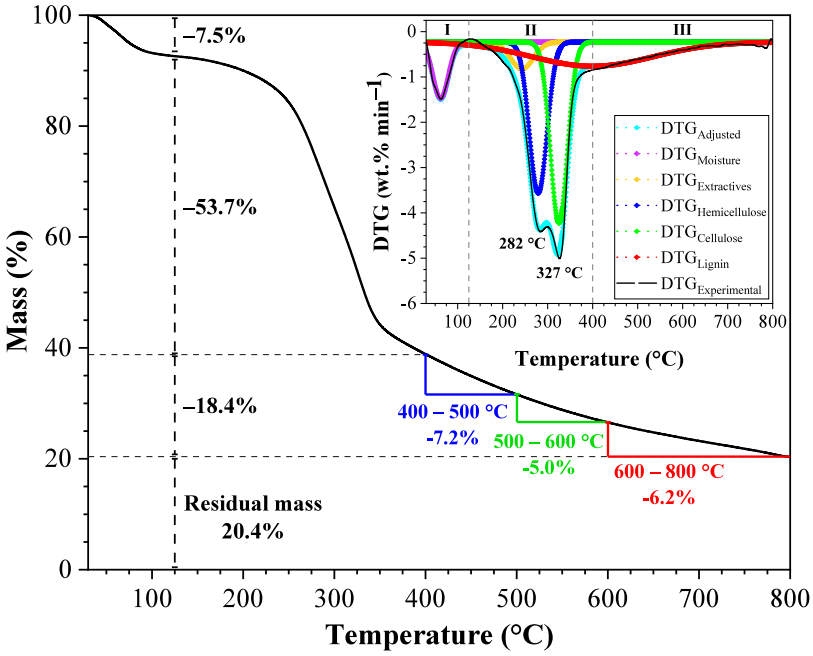

Figure 1. TGA and DTG curves of green coconut husk-derived biomass.

universal gas constant (0.082 atm L mol^{-1} K^{-1}), and m_{GCH} is the mass of biomass used during the pyrolysis process.

2.4.4. Determination of the Total Acidity Number of Bio-Oils. The acidity of the bio-oils was determined according to ASTM D974-22 (2023) and reported as the total acidity number (TAN). For the analysis, approximately 50 mg of the bio-oil sample was dissolved in 25 mL of a mixture of toluene, isopropanol, and deionized water in a 100:99:1 (v/v) ratio. The samples were titrated with a 0.01 mol L^{-1} KOH solution in isopropanol, previously standardized with potassium hydrogen phthalate. All analyses were performed in triplicate, and the TAN results are presented in $mg_{KOH}/g_{Bio\text{-}oil}$.

2.4.5. Total Phenolic Content Determination. The total phenolic content of the bio-oil samples was determined using the Folin-Ciocalteu (FC) method, following the procedure described by Stankovikj et al.[31] Stock solutions of bio-oils were prepared at a concentration of approximately 0.5 mg mL^{-1}, using a 1:1 (v/v) water/ethanol mixture as the solvent. A 40 μL aliquot of the stock solution was then transferred to a vial containing 3.16 mL of deionized water. Next, 0.2 mL of Folin-Ciocalteu reagent (Dinâmica Química, Brazil) was added, followed by 0.6 mL of a 20% (m/v) Na_2CO_3 aqueous solution. The final mixture was incubated at room temperature for 2 h to allow color development.

The solution was analyzed using a V-M5 spectrophotometer (Bel Photonics, Brazil), with absorbance measured at 765 nm. For quantification, a six-point calibration curve was prepared, covering concentrations from 0.1 a 1.0 mg mL^{-1}, using gallic acid as the standard. Analyses were performed in triplicate, and results were expressed as gallic acid equivalents (GAE).

2.4.6. Determination of Reducing Sugar Content of Bio-Oils. The total reducing sugar content in the bio-oil samples was determined using the traditional 3,5-dinitrosalicylic acid (DNS) method, with the DNS reagent prepared as described by Gonçalves et al.[32] After preparing the reagent, solutions of the bio-oils were made by diluting approximately 25 mg of bio-oil in 5 mL of a water:ethanol mixture (1:1 v/v). For the analysis, 500 μL of the bio-oil solution was transferred to a 5 mL glass vial, and 500 μL of the DNS solution was added. The mixture was heated in a water bath at 90 °C for 5 min, then the reaction was stopped by placing the vials in an ice bath for 5 min. The reaction mixture was subsequently diluted with 4 mL of deionized water.

The final solution was analyzed by spectrophotometry in the visible region, with absorbance measured at 540 nm. Reducing sugars were quantified using a calibration curve constructed with glucose standard solutions in the concentration range of 0.1 a 1.0 mg mL^{-1}. All analyses were performed in triplicate, and the results were expressed as glucose equivalents (GLE).

2.4.7. Thermogravimetric Analysis and Viscosity Assessment. The volatilization profile of the bio-oils obtained at different pyrolysis temperatures was determined by TGA analysis, using the system described in section 2.2.3. For the analysis, approximately 10 mg of each sample was heated from 30 to 600 °C at a heating rate of 10 °C min^{-1}. During the heating process, 10 min isothermal steps were applied at 100, 200, 300, 400, 500, and 600 °C, allowing assessment of the gradual volatilization of the compounds present in the bio-oils within specific temperature ranges.

The viscosity profile of the pyrolytic oils was assessed using rheological analysis. As these are Newtonian fluids, meaning their viscosity remains constant regardless of the applied shear rate,[33] the bio-oils were analyzed at a single shear rate of 10.0 s^{-1}. The rheological analyses were performed using a modular compact rheometer, model MCR-302 (Anton Paar, Austria), with a cone−plate geometry (25 mm diameter, 1° angle, and 52 μm truncation). Measurements were conducted over a temperature range of 20 to 50 °C.

2.4.8. Characterization of the Volatile Organic Fraction of Bio-Oils by GC/MS. For chromatographic analysis, bio-oil solutions were prepared in THF at a concentration of 15 mg mL^{-1}. These solutions were then derivatized using *N*,*O*-bis(trimethylsilyl)-trifluoroacetamide (BSTFA) as the derivatizing agent. Specifically, 20 μL of BSTFA was added to a 200 μL glass insert, followed by 60 μL of the bio-oil solution. The mixture was hermetically sealed and heated in a conventional microwave oven for four 10-s cycles, with 1 min intervals between each cycle. The analytical procedure was performed in triplicate. The derivatized solutions were analyzed using the GC/MS system described in section 2.2.2, and under the analytical conditions described by Silva et al.[17]

3. RESULTS AND DISCUSSION

3.1. Properties of Dry Biomass

3.1.1. Proximate and Elemental Characteristics. The results of the dried biomass characterization by proximal and elemental analysis are presented in Table S1. After the drying process, the moisture content of the biomass decreased from

https://doi.org/10.1021/acs.energyfuels.5c06504
Energy Fuels XXXX, XXX, XXX−XXX

76.5% (in natura) to 7.9%, a value suitable for use in the pyrolytic process (≤10%).[34] The ash content was 4.1%, classified as low according to Puri et al.[35] which is beneficial for biomass application in pyrolysis, as the effects of inorganic materials can be minimized. The volatile material (69.1%) and fixed carbon (26.8%) contents are consistent with values reported in the literature for coconut husk biomass,[3,36] with the former positively correlated with bio-oil yield and the latter with biochar production.

The elemental analysis of GCH showed percentages of C, H, N, and O similar to those reported in the literature for the same biomass, particularly when compared to the values from Fatmawati et al.[36] The biomass is composed mainly of carbon and oxygen, with percentages of 50.33 and 42.12%, respectively. Additionally, the H/C molar ratio of approximately 1.65 suggests a predominance of carbon chain structures with a naphthenic character, typical of the biomass polysaccharide matrix.[37] The O/C molar ratio of about 0.63 indicates a high presence of oxygenated functional groups, which is directly related to the lignocellulosic nature of the raw material.

The vegetable oil content of the GCH waste was 3.93% (m/m). The chromatographic analysis of the extracted oil by GC/MS showed a predominance of triglycerides composed of lauric ($C_{12:0}$), myristic ($C_{14:0}$), palmitic ($C_{16:0}$), and oleic ($C_{18:1}$) acids, with area percentages of 50.8, 17.0, 12.4, and 10.4%, respectively. Since triglyceride-based materials, when subjected to thermal conversion, typically generate liquid compound yields over 70%, containing mostly free fatty acids, determining the vegetable oil content in biomass waste is a relevant parameter. During the pyrolytic process, the fatty acids formed become part of the oil phase of the pyrolysis of the vegetable biomass, significantly influencing the yield, composition, and properties of the resulting bio-oil.[38,39]

3.1.2. TGA Analysis. Thermogravimetric analysis provided relevant information on the thermal degradation profile of GCH waste, as well as its compositional characteristics. The TGA and DTG curves of GCH biomass are shown in Figure 1.

The thermogravimetric behavior of the biomass can be divided into three distinct stages of thermal degradation. The first stage occurs at $T \leq 125$ °C, with a mass loss of approximately 7.5%. This initial loss is associated with the release of residual moisture from the biomass and the volatilization of low molecular mass compounds, consistent with the moisture content determined by immediate analysis. The second stage of degradation occurs between 150 and 400 °C, corresponding to the region with the highest percentage of mass loss (53.7%). In this temperature range, most of the decomposition of the biomass polysaccharide matrix takes place, along with partial degradation of lignin, as shown in the DTG curve in Figure 1. This process is evidenced by peaks in the DTG curve at approximately 282 and 327 °C, which are related to the degradation of hemicellulose and cellulose, respectively.[17] The third stage of thermal degradation occurs from 400 to 800 °C. In this temperature range, a mass loss of 18.4% is observed, attributed to the continued decomposition of lignin, which results in the release of volatiles and the formation of fixed carbon.[37] This material, together with the ash content of the biomass, contributes to a final residue from the thermogravimetric analysis equivalent to 20.4%.

About the lignocellulosic composition of GCH biomass, the results estimated from the TGA curves are shown in Table 1.

Table 1. Estimated Lignocellulosic Composition for GCH Biomass

component	this work[a]	Nascimento et al.[40]	Padilha et al.[41]	de Araújo et al.[42]
extractables (wt %)	5.5	–	16.5	14.2
hemicellulose (wt %)	23.9	25.5	15.9	14.7
cellulose (wt %)	27.8	31.6	28.8	33.0
lignin (wt %)	42.9	35.1	37.7	36.0

[a]Estimated by TGA analysis.

It was observed that the GCH residue from this study consisted mainly of lignin (~43%), followed by cellulose (~28%), hemicellulose (~24%), and extractable components (~5%). It is important to note that, although the results are estimated values, they are in agreement with the values presented in the literature for the same biomass.[40−42] In addition, the high lignin content is consistent with the high percentage of fixed carbon observed, since the thermal degradation of lignin occurs slowly and over a wide temperature range, contributing to the formation of fixed carbon during the thermal conversion process.[43]

Pyrolysis is a thermochemical process typically conducted at temperatures between 400 and 600 °C. As shown in Figure 1, among the components of lignocellulosic biomass, lignin is the main constituent affected within this temperature range, since pyrolysis temperatures above 400 °C promote greater degradation of this polymer. Analyzing the mass losses in this range, at 400 °C, the solid material from the TG analysis represented 38.8% of the mass. When the temperature increased to 500 °C, an additional 6.8% of volatiles were released, reducing the residue to 32%. At 600 °C, the residual mass decreased to 27%, corresponding to a further release of 5% volatiles. The increased degradation of biomass with rising temperature significantly affects the yield and composition of the pyrolysis products, supporting the study of different thermal conditions to optimize biomass processing.

3.2. Pyrolytic Products Yields

The distribution of the products obtained during the pyrolytic processing of GCH at different pyrolysis temperatures (400, 500, and 600 °C) is shown in Figure 2. The data showed a strong influence of temperature on the yields of pyrolysis products.

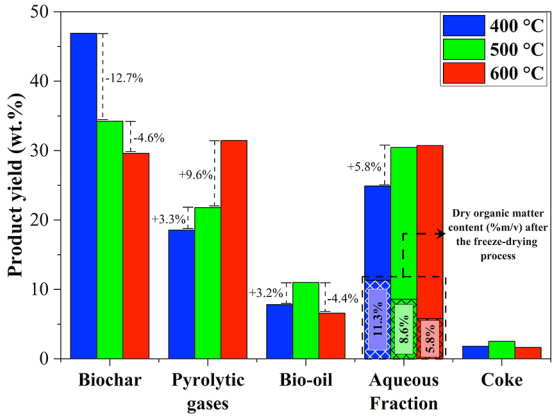

Figure 2. Pyrolysis product yields at different processing temperatures.

https://doi.org/10.1021/acs.energyfuels.5c06504
Energy Fuels XXXX, XXX, XXX−XXX

The biochar yield decreased from 46.9 to 29.6% between 400 and 600 °C, with a larger reduction between 400 and 500 °C (about 13 percentage points). This result aligns with the thermal degradation process of biomass, which is favored at higher temperatures and consequently leads to lower biochar production.[23] In addition, as observed in the TGA analysis, increasing the temperature significantly impacts the degradation of the lignin structure, one of the main factors responsible for char formation during biomass pyrolysis.[37,44]

On the other hand, increasing the pyrolysis temperature led to greater gas production, rising from 18.5% at 400 °C to 21.8% at 500 °C and 31.4% at 600 °C. This behavior is expected, since at higher temperatures the lignocellulosic matrix of the biomass undergoes greater degradation, releasing more chemical species in the volatile/gas phase.[45] In addition, the increased gas production between 500 and 600 °C is related to the occurrence of secondary cracking routes of the pyrolytic vapors, which aligns with the variation in bio-oil production as a function of pyrolysis temperature. Bio-oil yields increased from 7.8% at 400 °C to 11.0% at 500 °C, then decreased to 6.6% at 600 °C. This behavior indicates that a higher biomass degradation rate at 500 °C promotes increased formation of condensable volatile species; however, more intense energy conditions at 600 °C cause secondary degradation of organic compounds in the vapor phase, resulting in greater gas production and a reduction in bio-oil during the process.[46,47]

For the aqueous fraction, the product yield increased from 400 to 500 °C but remained nearly constant at 600 °C. In general, the water formed during the pyrolysis of lignocellulosic biomass has two main origins: the residual moisture of the raw material and the water generated by dehydration reactions.[47,48] Considering that the initial moisture content remained constant between experiments, the increase in the yield of the aqueous phase as the temperature increased suggests a greater occurrence of dehydration reactions under more severe thermal conditions, resulting in the additional production of water and, consequently, an increase in this fraction. Although the aqueous fraction contains polar organic compounds, the hypothesis of greater water formation was supported by analysis of the freeze-dried fraction, which showed a reduction in organic material content from 11.3% to 5.8% (m/v) between 400 and 600 °C. Although some volatile organic compounds may be lost during freeze-drying, the observed reduction in dry organic material content indicated a higher proportion of water in the products obtained at higher temperatures. At 600 °C, despite the yield being similar to that at 500 °C, the lower organic content reinforces the predominance of secondary dehydration reactions, which contributes to the simultaneous reduction in bio-oil yield.

In general, the influence of pyrolysis temperature on product yield in this study is similar to the effects observed by our research group in previous studies on the pyrolysis of cassava crop residues[17] and water hyacinth biomass.[49] Additionally, the results align with the general trends reported for the pyrolytic processing of lignocellulosic biomass at different temperature ranges.[20]

3.3. Biochar Characteristics

3.3.1. Physical-Chemical Properties. The physical and chemical properties of the biochars produced from GCH waste are shown in Table 2.

Table 2. Physicochemical Properties of Biochars Produced at Different Pyrolysis Temperatures

property	GCH	$BC_{400°C}$	$BC_{500°C}$	$BC_{600°C}$
proximate analysis				
moisture (m/m %)	7.9 ± 0.7	6.6 ± 0.2	3.7 ± 0.1	3.6 ± 0.1
volatile matter (m/m %)	69.1 ± 0.6	32.5 ± 0.5	19.6 ± 0.3	8.9 ± 0.2
ash (m/m %)	4.1 ± 0.7	8.9 ± 0.6	11.0 ± 0.7	13.0 ± 0.3
fixed carbon[a] (m/m %)	26.8 ± 0.8	58.6 ± 0.7	69.4 ± 0.7	78.1 ± 0.1
elemental analysis				
C[b] (m/m %)	50.33 ± 0.34	70.05 ± 0.30	78.83 ± 0.03	84.10 ± 0.17
H[b] (m/m %)	6.92 ± 0.20	5.13 ± 0.04	3.98 ± 0.01	2.93 ± 0.04
N[b] (m/m %)	0.64 ± 0.01	1.50 ± 0.01	1.49 ± 0.03	1.39 ± 0.06
O[c] (m/m %)	42.12 ± 0.5	23.32 ± 0.33	15.7 ± 0.02	11.58 ± 0.07
HHV (MJ kg^{-1})	21.7	28.0	30.4	31.6
H/C (molar ratio)	1.65	0.88	0.61	0.42
O/C (molar ratio)	0.63	0.25	0.15	0.10
N/C (molar ratio)	0.011	0.018	0.016	0.014
FC/C_{total}	–	83.7%	88.0%	92.9%
pH	–	5.67 ± 0.03	7.78 ± 0.02	8.06 ± 0.01
inorganic content (% by EDX analysis)				
K	0.96	0.99	3.39	3.72
Cl	0.84	0.79	2.51	2.84
Ca	0.07	0.07	0.26	0.27
P	0.05	0.07	0.22	0.23

[a]Obtained by difference on a dry basis. [b]Dry and ash-free basis. [c]Obtained by difference.

The results of the proximate analyses showed that moisture and volatile material content tended to decrease as pyrolysis temperature increased, favoring the production of biochars with higher percentages of fixed carbon and ash. The reduction in volatile material content in biochar is related to the fact that higher temperatures promote greater degradation of the biomass, resulting in less functionalized biochars with higher fixed carbon content (more hydrophobic).[47] In addition, the increase in ash content is due to the concentration of inorganic minerals in the biochar, as the yield decreases at higher pyrolysis temperatures and these minerals become more concentrated in the solid matrix.[23]

For the elemental analysis, it was observed that increasing the pyrolysis temperature produced biocoals with higher carbon content, rising from 70.0% at $BC_{400°C}$ to 84.1% at $BC_{600°C}$. In addition, there was a significant reduction in hydrogen (from 5.1 to 2.9%) and oxygen (from 23.3 to 11.6%) contents, while nitrogen showed a slight decrease (from 1.5 to 1.4%). These results corroborate the data from the proximate analysis, as the decrease in hydrogen, oxygen, and nitrogen content is related to the defunctionalization of the carbonaceous matrix. This process releases components in the volatile phase during pyrolysis through dehydration, deoxygenation, and demethylation reactions, favoring the formation of a matrix rich in condensed aromatic carbon.[47]

The increase in aromatization was demonstrated by the reduction in H/C ratio values as the pyrolysis temperature increased, from 0.88 at 400 °C to 0.42 at 600 °C, confirming the formation of biochar with a higher content of aromatic structures.[50] Similarly, the O/C molar ratio decreased from 0.25 ($BC_{400°C}$) to 0.10 ($BC_{600°C}$), indicating that biochar produced at higher temperatures contained fewer oxygenated

https://doi.org/10.1021/acs.energyfuels.5c06504
Energy Fuels XXXX, XXX, XXX−XXX

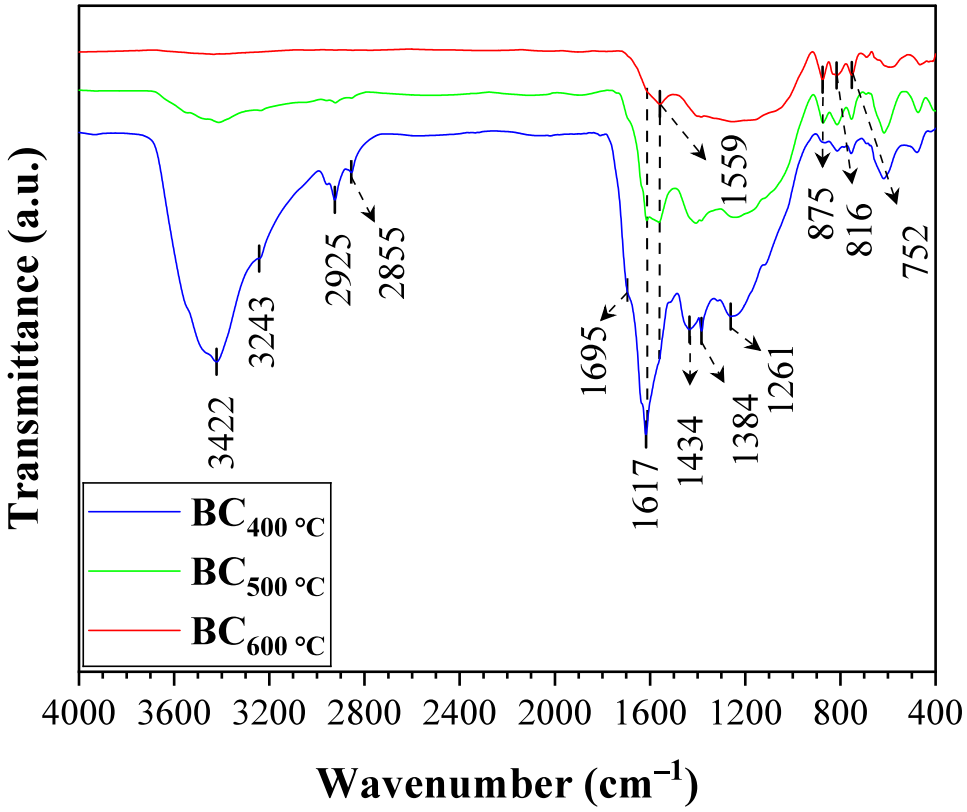

Figure 3. FTIR spectra of GCH biochars at different temperatures.

functional groups, such as hydroxyl and carboxylic groups, in its structure. This result was supported by the increase in the pH values of the biochars ($BC_{400°C}$: pH 5.67, $BC_{500°C}$: pH 7.78, and $BC_{600°C}$: pH 8.06), which is related to the degradation of acidic groups in the biochar, as well as the rise in ash content as the pyrolysis temperature increased.[27,51] Regarding the N/C ratio, there was a slight reduction from 0.018 at 400 °C to 0.014 at 600 °C, suggesting greater thermal resistance of the nitrogen functional groups, possibly due to the presence of nitrogen in aromatic heterocyclic structures.

Considering the application of biochars to soil as an agricultural input and a form of carbon sequestration, Balmuk et al.[52] related the O/C values to biochar stability, reporting that biochars with an O/C ratio below 0.2 have a half-life of over 1,000 years, while O/C ratios in the 0.2−0.6 range have half-lives between 100 and 1,000 years. The results obtained show that biochars produced at 500 and 600 °C may have greater environmental stability, as corroborated by the FC/C_{total} index values, which represent the stable carbon fraction of the biochar. Approximately 88 and 93% of the carbon present in the biochars produced at 500 and 600 °C, respectively, corresponds to stable carbon, supporting the potential use of these biochars as carbon sequestration agents. In addition, analysis of inorganic elements in the samples showed an increase in the percentage of K, Cl, Ca, and P in the biochars produced at higher temperatures. Other elements such as S, Fe, Cu, and Zn were also detected, but their concentrations were below the equipment's quantification limit. Since K, Ca, and P are essential macro- and micronutrients for plant development, the higher levels of these elements in the biochars produced at 500 and 600 °C suggest that these materials are more suitable as inputs for improving the quality of agricultural soils.[53]

3.3.2. Assessment of the Functional Groups of the Biochars. The functional groups present in the biochars produced were identified using FTIR analysis. The spectra acquired are shown in Figure 3.

The results showed a significant influence of pyrolysis temperature on the functional groups present in the biochars produced. The most notable change was a reduction in the intensity of the band around 3600 to 3200 cm^{-1}, corresponding to the stretching vibration of the O−H bond in phenolic compounds and conjugated carboxylic groups (COOH). The presence of carboxylic groups is confirmed by signals corresponding to the stretching of the C═O bond (1695 cm^{-1}) and the asymmetric stretching of COO bonds (1617 cm^{-1}).[54,55] The decrease in the intensity of these signals with increasing pyrolysis temperature supports the observed increase in pH of solutions with biochars produced at higher temperatures, indicating that higher temperatures promote the degradation of acidic structures containing hydroxyl and carboxyl groups through dehydration and decarboxylation.[22,23] Additionally, a reduction in the signals around 2925 and 2855 cm^{-1} was observed, corresponding to the asymmetric and symmetric stretching vibrations of sp^3 carbon C−H bonds, respectively, as the pyrolysis temperature increased from 400 to 600 °C. This may be related to the cleavage of C−C bonds in aliphatic chains or the demethoxylation of lignin derivatives.[22,56]

Increasing the pyrolysis temperature resulted in biochars with carbonaceous structures containing fewer oxygenated functional groups, as confirmed by the general reduction in the intensities of the bands located between 1400 and 1000 cm^{-1}. This effect is mainly attributed to the elimination of hydroxyl groups and the cleavage of C−O bonds. The deoxygenation

https://doi.org/10.1021/acs.energyfuels.5c06504
Energy Fuels XXXX, XXX, XXX−XXX

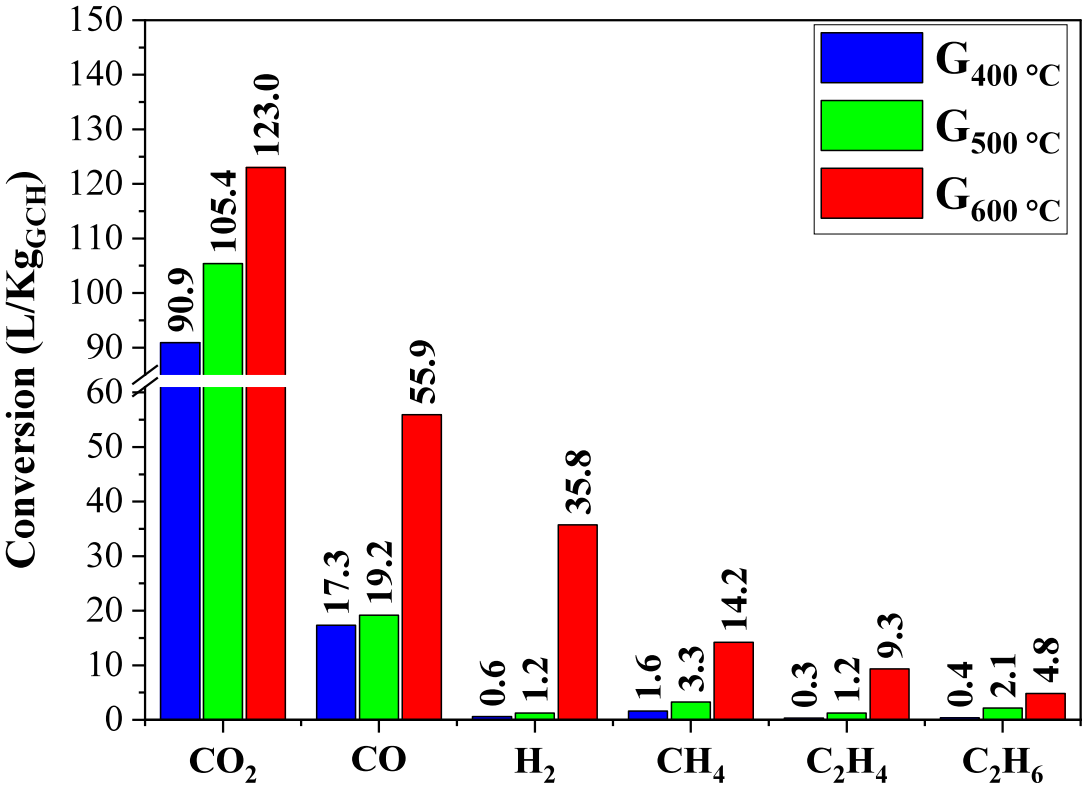

Figure 4. Gaseous species distribution produced by the pyrolysis of GCH biomass.

reaction pathways promoted at higher temperatures produced biochars with more aromatic structures,[23] especially for the biochar produced at 600 °C, which is consistent with the elemental analysis results shown in Table 1. This is further supported by the presence of bands between approximately 1600 and 1450 cm^{-1}, associated with C=C stretching of aromatic rings, as well as bands in the range of 900 to 700 cm^{-1}, which indicate out-of-plane bending of the C−H bonds in aromatic rings.[22]

3.4. Characteristics of Pyrolytic Gases

Analysis of the noncondensable products revealed the following gases in their composition: CO_2, CO, H_2, CH_4, C_2H_4 e C_2H_6. The behavior of the gas composition as a function of pyrolysis time is shown in Figure S2 of the Supporting Information. It was observed that after the start of the experiment, between 5 and 30 min, the analyzed gases showed relatively stable compositions over time, with deviations from the average (dashed lines) in most analyses of less than 20%. This result indicates that the process maintained stable behavior over the experimental period. This pattern was verified at all evaluated temperatures (400, 500, and 600 °C), reinforcing the operational stability of the system during the pyrolysis of biomass derived from GCH.

When analyzing the average composition, it was observed that the gaseous product of pyrolysis at 400 and 500 °C consisted mainly of CO_2 and CO, with similar percentages at both temperatures, ∼80% for CO_2 and ∼15% for CO. H_2 and light hydrocarbons (CH_4, C_2H_4, and C_2H_6) accounted for less than 2.5%. Pyrolysis at 600 °C resulted in a decrease in the CO_2 percentage (from ∼80% at 400 and 500 °C to ∼50%). At the same time, there was a significant increase in the percentages of CO (from ∼15 to ∼23%), H_2 (from less than 1 to ∼15%), and light hydrocarbons (from less than 5 to ∼12%). These results indicate that at temperatures ≤500 °C, the predominant reaction mechanisms are mainly associated with the degradation of oxygenated groups in the lignocellulosic matrix, like decarboxylation pathways releasing CO_2 and decarbonylation or C−O−C bonds cleavage, releasing CO, while aromatization mechanisms (release of H_2) and cleavage of C−C bonds (release of light hydrocarbons) are less favored. At 600 °C, the energy conditions favor the occurrence of secondary aromatization mechanisms and the cleavage of C−O−C and C−C bonds, leading to the formation of CO and gaseous hydrocarbons, respectively.[37]

Although the molar composition analysis indicates a reduction in CO_2 formation as the pyrolysis temperature increases, this result should be interpreted as a relative reduction, due to the increased formation of other constituents in the pyrolysis gases, and not necessarily as a decrease in the absolute volume of CO_2 generated. To better assess this, each gas species was quantified during the pyrolysis of the biomass at different temperatures, with the results expressed on a volumetric basis as shown in Figure 4. The representation of the data on a mass basis has also been calculated and is available in Table S2 of the Supporting Information.

When comparing the processes at 400 and 500 °C, it was observed that, in absolute terms, gas production increased, especially CO_2, which rose from ∼91 L kg^{-1} in pyrolysis at 400 °C to ∼105 L kg^{-1} at 500 °C. When correlated with the product yields, the increase in CO_2 production may result from the decarboxylation of COOH groups in the biochars, reducing their yield at 500 °C and consequently increasing gas production. This hypothesis aligns with the reduction in oxygen content of the biochars produced at higher temperatures, the increase in pH values, and the reduction in the intensity of the band associated with the stretching vibration of

https://doi.org/10.1021/acs.energyfuels.5c06504
Energy Fuels XXXX, XXX, XXX−XXX

O−H bonds at 3600−3200 cm^{-1}, the band around 1700 cm^{-1} related to C═O bond stretching, and the signal at 1617 cm^{-1} associated with the asymmetric stretching of COO bonds of acids, as discussed earlier. In addition, the data indicate that at 500 °C, the energy conditions were not favorable for the secondary degradation of pyrolysis vapors, limiting the formation of gases such as CO, H_2 and light hydrocarbons. As a result, the greater degradation of the solid phase was directly reflected in the increase in bio-oil production.

For the 600 °C process, there was a significant increase in the production of all components in the mixture, including CO_2, which increased from ∼105 L kg^{-1} at 500 °C to 123 L kg^{-1} at 600 °C. The most pronounced increases were observed for CO (from ∼19 to ∼56 L kg^{-1}) and H_2 (from 1.2 to ∼36 L kg^{-1}). Additionally, there were significant increases in the production of light hydrocarbons, with a total yield of 28.3 L kg^{-1}. These results indicate that the 600 °C energy condition favored the cracking of the pyrolysis steam phase through decarboxylation mechanisms, producing CO_2; cleavage of C−O−C bonds in lignin derivatives and decarbonylation, leading to CO formation; aromatization routes, responsible for the increase in H_2; and cracking of C−C bonds and demethoxylation, which favored the production of light hydrocarbons.[37,45,57]

3.5. Properties of Bio-Oils

3.5.1. Elemental Composition. The results obtained through the elemental analysis of the bio-oils produced are available in Table 3.

Table 3. Elemental Composition of GCH Bio-Oils

parameter	GCH	$BO_{400°C}$	$BO_{500°C}$	$BO_{600°C}$
C (m/m %)	50.33 ± 0.34	52.73 ± 0.95	60.76 ± 0.09	67.12 ± 0.52
H (m/m %)	6.92 ± 0.20	9.39 ± 0.30	9.19 ± 0.03	8.53 ± 0.07
N (m/m %)	0.64 ± 0.01	0.77 ± 0.03	0.94 ± 0.01	1.42 ± 0.01
O[a] (m/m %)	42.12 ± 0.50	37.11 ± 0.64	29.12 ± 0.06	22.93 ± 0.47
H/C (molar ratio)	1.65	2.14	1.81	1.52
O/C (molar ratio)	0.63	0.53	0.36	0.26
N/C (molar ratio)	0.011	0.013	0.013	0.018
water content (m/m %)	–	26.8 ± 1.9	11.5 ± 0.9	7.6 ± 0.9
HHV (MJ kg^{-1})	21.7	25.9	29.2	31.1

[a]Obtained by difference.

Increasing the pyrolysis temperature produced bio-oils with a higher carbon content and lower oxygen content, along with a slight reduction in hydrogen between 400 and 500 °C, which became more pronounced at 600 °C. These results show that the use of higher temperatures increased the degree of unsaturation in the bio-oils, as indicated by the reduction in the H/C ratio from 2.14 ($BO_{400°C}$) to 1.52 ($BO_{600°C}$). Similarly, there was a decrease in the O/C ratio, from 0.53 ($BO_{400°C}$) to 0.26 ($BO_{600°C}$), indicating the formation of bio-oils with a lower content of oxygenated functional groups. These results are in line with the reduction in water content observed in the bio-oils, which decreased from 26.8% at $BO_{400°C}$ to 11.5% at $BO_{500°C}$ and 7.6% at $BO_{600°C}$. The promotion of the deoxygenation and aromatization pathways at higher pyrolysis temperatures contributed to an increase in the hydrophobic character of the bio-oil, thus reducing its interaction with water molecules.

By correlating the reduction in the percentages of oxygen and hydrogen with the yields of pyrolysis products and gas analyses, it is observed that increasing the temperature favors deoxygenation mechanisms, contributing to the reduction of oxygen content in solid and liquid products. Additionally, higher temperatures intensify dehydration pathways, promoting the reduction of hydroxyl groups (−OH) in the products and resulting in an increased proportion of water in the aqueous fraction. Higher temperatures also promote cracking, demethoxylation, and aromatization mechanisms, converting oxygenated species into more aromatic or unsaturated molecules rich in carbon.[37,45,57] Finally, the increase in nitrogen content suggests that nitrogenous compounds tend to remain in the liquid product, as they were not completely converted into gases or biochar within the temperature range studied.

When comparing the higher calorific value of bio-oils with GCH biomass, it is observed that the HHV values increase from 25.9 to 31.1 MJ kg^{-1} between 400 and 600 °C, which is higher than that of the biomass (21.7 MJ kg^{-1}) and also higher than what is generally reported for bio-oils from lignocellulosic biomass.[17,49,58] This result may be related to the lipid content of the biomass which, as mentioned above, during the thermochemical process tends to concentrate in the oily product of the pyrolysis. In addition, the high lignin content may also favor the formation of bio-oils with a higher energy density, since lignin, due to its lower degree of oxygenation, has a higher HHV than holocellulose polymers.[59−61] Thus, the compounds generated from its thermal decomposition contribute to increasing the calorific value of bio-oils, demonstrating the high energy potential of the product.

3.5.2. Determination of the Acidity Index and Total Phenolic and Reducing Sugar Content of Bio-Oils. The

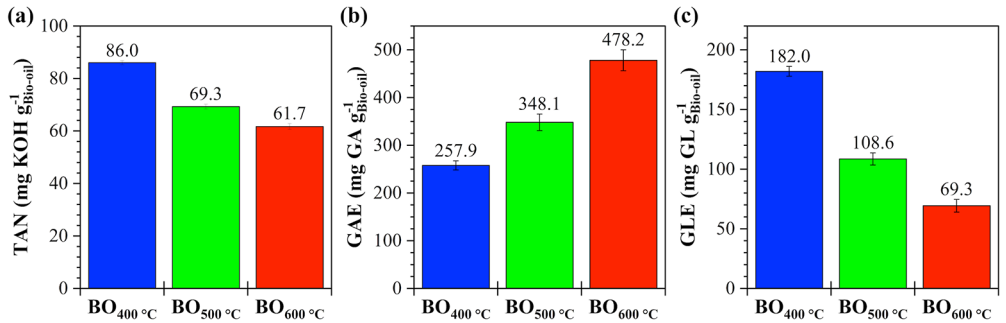

Figure 5. Total acidity number (a), total phenolic content (b), and total reducing sugars (c) of the bio-oils produced at different pyrolysis temperatures.

https://doi.org/10.1021/acs.energyfuels.5c06504
Energy Fuels XXXX, XXX, XXX−XXX

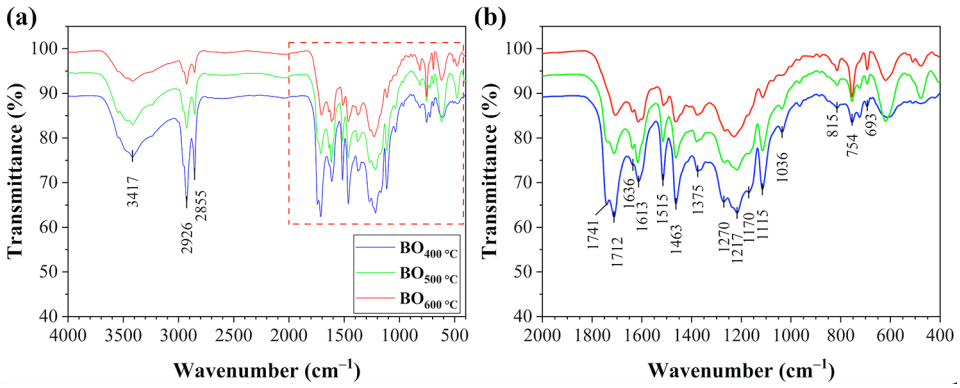

Figure 6. FTIR spectra of GCH bio-oils at different temperatures: (a) full spectra and (b) region magnification between 2000 and 400 cm^{-1}.

results obtained by determining the total acidity number (TAN), total phenolic content and reducing sugar content for the bio-oil samples are shown in Figure 5.

The analysis of the effects of pyrolysis conditions on the bio-oil showed that increasing the temperature directly affected the acidity of the matrix, as well as the phenolic and sugar contents in the product. Generally, higher temperatures produce bio-oils with lower TAN values and lower levels of reducing sugars, but higher concentrations of phenolic compounds. Specifically, the bio-oils exhibited TAN values ranging from 86 mg_{KOH} g^{-1} at 400 °C to about 62 mg_{KOH} g^{-1} at 600 °C. The levels of reducing sugars decreased from 182 to 69.3 mg_{GL} g^{-1} as the temperature increase from 400 to 600 °C, while the content of phenolic compounds increased from approximately 258 mg_{AG} g^{-1} to about 478 mg_{AG} g^{-1} over the same temperature range.

The acidity of bio-oils from lignocellulosic biomasses mainly results from the presence of phenolic compounds and carboxylic acids, such as fatty acids.[31] Thus, although the increase in phenolics with rising temperature may also contribute to the product's acidity, the reduction observed in TAN values suggests that carboxylic acid species were more intensely degraded during processes at 500 and 600 °C. This behavior aligns with the increase in CO_2 and CO production observed at higher temperatures, which is characteristic of decarboxylation and decarbonylation processes.[62] In addition, the reduction in reducing sugar levels may be associated with dehydration mechanisms, which would explain the increase in the proportion of water in the aqueous fractions (section 3.2).[31,63,64] Furthermore, the increase in phenolic compound content with higher pyrolysis temperatures corroborates the more intense degradation of the biomass lignin matrix, leading to the formation of a more aromatic product rich in phenolics.[2]

3.5.3. Functional Groups Evaluation. The FTIR spectra of the bio-oils produced from GCH pyrolysis at different temperatures are shown in Figure 6.

In all bio-oils, a broad band between 3600 and 3200 cm^{-1} was identified, corresponding to the stretching of O−H bonds related to phenolic hydroxyls, carboxylic acids, and the presence of water in the samples.[22] As the pyrolysis temperature increased, a reduction in the intensity of this band was observed, suggesting that compounds containing hydroxyl groups tend to be converted under higher energy conditions. This interpretation is supported by the decrease in the band around 1712 cm^{-1}, associated with the stretching of C═O bonds in carboxylic acids,[65] indicating that higher temperatures favor decarboxylation mechanisms, with CO_2 released in the gas phase, thereby reducing, for example, the fatty acid content in the bio-oil. Additionally, this result aligns with the reduction in the acidity index of bio-oils produced at higher temperatures.

A similar trend is observed for the signals at 2926 and 2855 cm^{-1}, related to the asymmetric and symmetric stretches of the C−H bonds of sp^3 carbon.[17] The reduction in the intensity of these signals with increasing temperature suggests the occurrence of demethoxylation reactions of lignin derivatives or cleavage of C−C bonds in aliphatic chains.[56,66] The hypothesis of demethoxylation is reinforced by the decrease in the bands at 1270 and 1036 cm^{-1} (Figure 6b), associated with the stretching vibration of the C−O bonds of aryl ethers present in compounds such as guaiacol and syringol, which result from the degradation of lignin.[67] The hypothesis of C−C bond cracking may be associated with the cleavage of TAG chains, which is supported by the reduction of the stretch band of the C═O ester bond at around 1741 cm^{-1},[65] as well as by the decrease in signal intensity at 1463 cm^{-1}, associated with the bending of CH_2 groups.[68]

In addition, the bio-oils obtained at higher temperatures showed a lower band intensity at 1115 cm^{-1}, associated with the stretching of the C−O bond of aliphatic ethers present in cellulose and hemicellulose derivatives.[69] As the pyrolysis temperature increased, the intensity of this band decreased, indicating that higher temperatures reduced the content of aliphatic compounds derived from sugars in the bio-oil. This corroborates the results of the determination of reducing sugar content in the bio-oils.

The increase in pyrolysis temperature favored the formation of bio-oils with a higher content of aromatic species, as evidenced by the bands at 1613 and 1515 cm^{-1}, associated with the stretching of C═C bonds in aromatic compounds, as well as signals between 900 and 650 cm^{-1}, related to the out-of-plane bending of C−H bonds in aromatic rings, demonstrated, for example, by phenolic compounds present in the samples.[58] In addition, the signals between 1300 and 1000 cm^{-1} are attributed to the stretching of C−O bonds. The band at 1217 cm^{-1}, the most intense in this region, may be associated with phenolic structures, while the signal at 1170 cm^{-1} may be related to alcohols, as well as the C−O bonds of esters and acids, which can also exhibit stretching in this wavenumber range.[22,70]

3.5.4. Volatilization and Viscosity Profiles of Bio-Oils. The volatilization profile of the species comprising the GCH bio-oils was evaluated by measuring mass losses across different temperature ranges. The TGA curves from the analysis of pyrolytic oils produced at various pyrolysis

https://doi.org/10.1021/acs.energyfuels.5c06504
Energy Fuels XXXX, XXX, XXX−XXX

temperatures are shown in Figure S3. To facilitate data analysis and allow direct comparison between bio-oils, the mass loss values observed in each temperature range are presented in Table 4.

Table 4. Percentage of Mass Loss in Various Temperature Ranges for Bio-Oils Derived from Coconut Husks Pyrolysis

temperature range	$BO_{400°C}$	$BO_{500°C}$	$BO_{600°C}$
$T \leq 100$ °C	24.1%	30.5%	31.6%
100 − 200 °C	29.1%	30.2%	35.5%
200 − 300 °C	21.5%	19.0%	10.4%
300 − 400 °C	15.6%	9.0%	4.9%
400 − 500 °C	1.7%	1.9%	2.9%
500 − 600 °C	1.7%	2.0%	3.6%
total mass loss	93.7%	92.6%	88.9%
analysis waste (coke)	6.3%	7.4%	11.1%

Considering that at temperatures ≤200 °C, direct volatilization processes predominate with minimal thermal degradation, the data in Table 3 show that increasing the pyrolysis temperature favored the formation of lighter and more volatile compounds.[71] This effect is evidenced by the higher mass losses observed at $T \leq 200$ °C in samples obtained at higher temperatures (~67% ($BO_{600°C}$) > ~61% ($BO_{500°C}$) > ~53% ($BO_{400°C}$)). In the 200 to 300 °C range, bio-oils produced at lower temperatures released vapors more intensely (21.5% ($BO_{400°C}$) > 19% ($BO_{500°C}$) > 10.4% ($BO_{600°C}$)), suggesting a higher content of compounds that volatilize at higher temperatures.[72]

Between 300 and 400 °C, the mass losses occurred in the following order: 15.6% ($BO_{400°C}$) > 9.0% ($BO_{500°C}$) > 4.9% ($BO_{600°C}$). Above 300 °C, thermal degradation processes become more significant, promoting not only volatilization but also the cleavage of thermally unstable oligomeric structures. Thus, the data suggests that the bio-oils obtained at 500 and 600 °C have a lower oligomer content, resulting from greater thermal cracking of the biomass, which forms lighter and more volatile compounds. Above 400 °C, the most stable compounds in the bio-oils tend to undergo condensation mechanisms, leading to the formation of carbonaceous solid matrices (coke). The formation of this material increased in the most energetic processes, from 6.3% in $BO_{400°C}$ to 11.1% in $BO_{600°C}$, a behavior attributed to the higher degree of aromatization of the bio-oil, since polyaromatic compounds, due to their chemical stability, tend to polymerize and condense during heating, resulting in coke formation after volatilization and degradation of the other fractions.[73,74]

The increased volatility of the bio-oils produced at higher temperatures was reflected in their viscosity data, as shown in Figure 7.

Regarding viscosity, processes conducted at higher pyrolysis temperatures produced more fluid (less viscous) bio-oils, reflecting greater cracking of organic vapors during the process.[75] The viscosity of the bio-oils strongly depended on the analysis temperature, with reductions of approximately 75−80% when the temperature increased from 20 to 50 °C. However, in the range of 40 to 50 °C, the bio-oils produced by pyrolysis at 400, 500, and 600 °C exhibited similar viscosities, ranging from 24 to 35 mPa·s. This decrease occurs because higher temperatures increase the kinetic energy of the molecules, weakening intermolecular interactions and facilitating flow, resulting in less viscous fluids.[76] Compared to data in

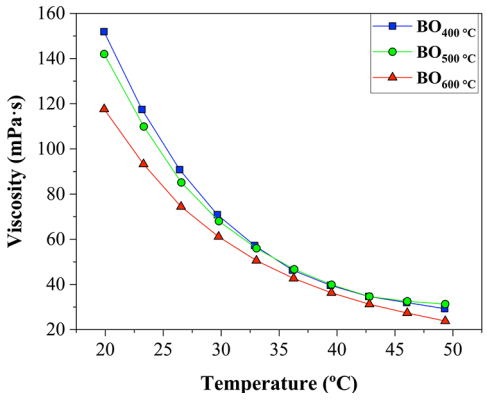

Figure 7. Viscosity profile of bio-oils according to temperature.

the literature, the bio-oils produced from green coconut husks in this work were more fluid than those obtained by pyrolysis at 500 °C from forest biomass, such as Norway spruce (~94 mPa·s at 40 °C), white pine (~118 mPa·s at 40 °C), poplar (~100 mPa·s at 40 °C), oak (~70 mPa·s at 40 °C), and beech wood (~97 mPa·s at 40 °C).[33,76,77]

3.5.5. Composition of the Bio-Oil Fraction Analyzable by GC−MS. The composition of the bio-oils was determined by GC−MS analysis, and the resulting Total Ion Current Chromatograms (TICCs) are presented in Figure S4. Visual evaluation of the chromatograms indicated similar profiles among the samples, with the same main compounds present, differing only in intensity. These differences were most noticeable in the highlighted peaks, especially for fatty acids and cresols (methyl-phenols), whose intensities decreased and increased, respectively, as the pyrolysis temperature increased.

From the chromatographic data, approximately 67, 66, and 67 compounds were identified in the samples produced at 400, 500, and 600 °C, respectively. Together, these compounds accounted for 90 to 95% of the total chromatogram area. The identified compounds were grouped into classes based on their main organic functions: carboxylic acids, phenolics (including phenol, alkylphenols, methoxyphenols, and hydroxyphenols), alcohols, hydrocarbons, monoglycerides, aldehydes, ketones, and furans. The chemical distribution of these compounds is shown in the class histogram in Figure 8, and Table S2 lists the identified compounds grouped by chemical class.

The main classes that composed the bio-oils are carboxylic acids, primarily fatty acids resulting from the cracking of biomass triglycerides, and phenolic compounds, mainly from the degradation of lignin. Among the main compounds in these classes in bio-oils produced at 400, 500, and 600 °C, lauric acid stands out with ~11% by area, and phenol monomer, which accounts for ~18%. The high amount of phenol in the bio-oils produced in this study is consistent with bio-oils derived from coconut shells studied by Kwon et al.[78] and Andrade et al.,[18] and is associated with the high lignin content in this type of biomass.

The increase in pyrolysis temperature led to a reduction in the percentage of carboxylic acids in the bio-oil, from ~42% ($BO_{400°C}$) to ~35% ($BO_{600°C}$). This result was mainly attributed to the degradation of long-chain fatty acids ($C_{14:0}$, $C_{16:0}$, $C_{18:2}$, $C_{18:1}$, and $C_{18:0}$), which together accounted for 25.4, 20.2, and 14.0% of the carboxylic acid content in bio-oils produced at 400, 500, and 600 °C, respectively. In addition to affecting fatty acids, the increase in pyrolysis temperature also reduced the monoglyceride content in the bio-oil. These

https://doi.org/10.1021/acs.energyfuels.5c06504
Energy Fuels XXXX, XXX, XXX−XXX

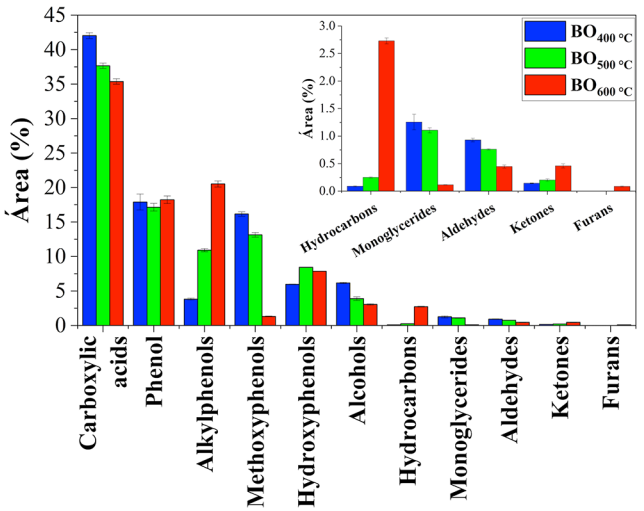

Figure 8. Composition of bio-oils according to the chemical classes identified by GC/MS.

findings support the hypotheses regarding a higher degree of thermal cracking at elevated temperatures and the reduction of the acidity index in samples as pyrolysis temperature increases. Through decarboxylation and decarbonylation mechanisms, these conditions may have favored increased hydrocarbon production in bio-oil produced at 600 °C.[62]

Regarding phenolic compounds, it was observed that increasing the pyrolysis temperature from 400 to 500 °C led to a rise in the relative content of lignin derivatives in the bio-oil, from ∼44% in $BO_{400°C}$ to ∼50% in $BO_{500°C}$. However, at 600 °C, the bio-oil produced showed a slightly lower phenolic content (around 48%). In contrast, the total phenolic content, determined by the Folin-Ciocalteu (FC) method, increased progressively with higher pyrolysis temperatures, a trend not observed in the data obtained by GC/MS. It is believed that the higher phenolic content determined by the FC method in the bio-oil produced at 600 °C is due to a greater proportion of polyaromatic phenolic compounds, whose formation is intensified at higher temperatures, as in $BO_{600°C}$.[37,79] These compounds, due to their low volatility and high molecular weight, are difficult to detect by GC, which may explain the discrepancy observed in the total phenolic content of the samples.[80] Additionally, the TGA analysis results supported this hypothesis, since polyaromatic structures can undergo polymerization during heating, resulting in the formation of coke, which was produced in greater quantity in the $BO_{600°C}$ analysis.

The main changes in the phenolic class occurred in the methoxyphenol and alkylphenol groups. The results show that increasing the pyrolysis temperature led to a progressive reduction in methoxyphenol content in the bio-oil, from ∼16% in $BO_{400°C}$ to ∼13% in $BO_{500°C}$ and 1.3% in $BO_{600°C}$. In contrast, the alkylphenol content increased from 3.8% ($BO_{400°C}$) to 10.9% ($BO_{500°C}$) and 20.5% ($BO_{600°C}$). These changes are associated with secondary mechanisms of demethoxylation and demethylation of methoxylated phenolics, especially guaiacol and syringol, which contribute to the release of gases such as CO and CH_4. These transformations result in the formation of hydroxyphenols, such as catechol, and subsequently alkylphenols, such as cresols (ortho-, meta-, and para-cresol), through alkylation reactions.[17,81,82]

The chemical characteristics of bio-oils derived from coconut husks demonstrate their high potential as sources of compounds of industrial interest. The significant presence of phenols, particularly monomeric phenol, indicates a viable alternative to phenol of petrochemical origin. The high concentration of fatty acids, especially at pyrolysis temperatures around 500 °C, a condition that maximizes bio-oil yield, further expands the possibilities for conversion into renewable hydrocarbons. Additionally, the compound profile can be adjusted by controlling the pyrolysis temperature, allowing optimization of the process to obtain specific chemical classes, such as alkylphenols, which reached high levels in the sample produced at 600 °C.

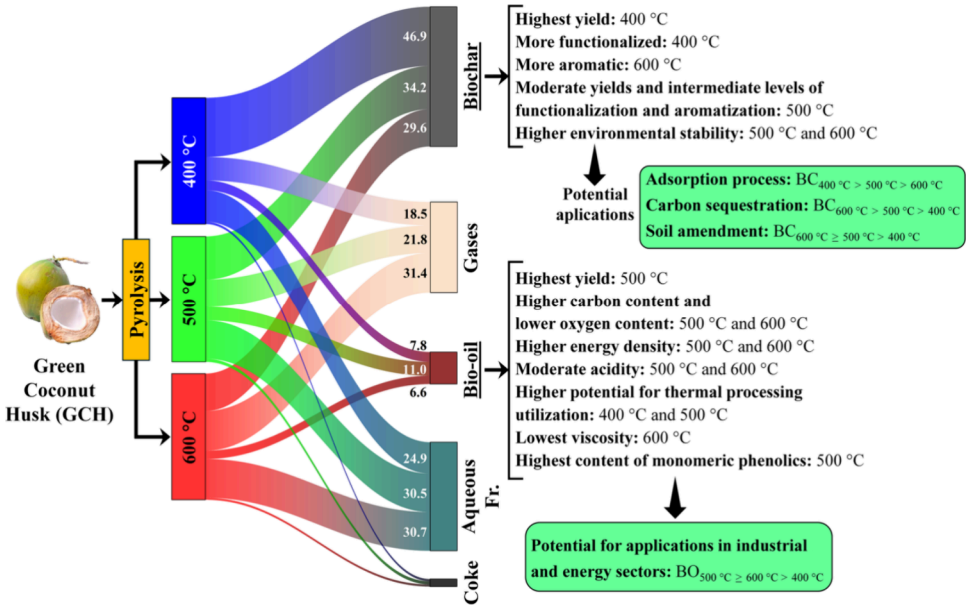

Figure 9. Sankey diagram for pyrolysis product yields and chemical properties of the main products obtained from GCH pyrolysis at 400, 500, and 600 °C.

https://doi.org/10.1021/acs.energyfuels.5c06504
Energy Fuels XXXX, XXX, XXX−XXX

3.6. Integrated Analysis of the Yields and Chemical Properties of the Products

The yields of the products obtained during pyrolysis at different temperatures were correlated with their chemical characteristics to identify the optimal condition for processing green coconut shells and the potential applications of the main products. Figure 9 provides a general analysis of the most relevant characteristics of the main products obtained under each processing condition.

Biochar produced at 400 °C showed higher yield and a greater degree of functionalization, making it more promising for adsorption applications.[83] In contrast, biochar produced at 600 °C exhibited a more aromatic structure, lower content of oxygenated functional groups, high fixed carbon content, and high stability; desirable properties for carbon sequestration.[52] Processing biomass at 500 °C resulted in biochar with intermediate yield and chemical characteristics in terms of functionalization and aromatization compared to materials obtained at 400 and 600 °C. This biochar also demonstrates good environmental stability due to its high fixed carbon content and can be used for a wider range of applications, including adsorption processes, soil applications, and carbon sequestration, thereby expanding the potential for valorization of coconut husk-derived raw material.

Regarding the bio-oils, pyrolysis at 500 °C resulted in the highest yield of this product, with carbon and oxygen contents similar to those observed in the bio-oil obtained at 600 °C, as well as a high energy density. Additionally, the bio-oil generated at 500 °C showed moderate acidity, significantly lower than that observed in the bio-oil produced at 400 °C, making it more promising for energy applications. Since the processing of pyrolytic oils for renewable fuel formulation involves thermal and thermocatalytic steps, it is notable that, compared to the process at 600 °C, the oil produced at 500 °C had a lower concentration of condensed polyaromatic compounds (coke precursors), indicating greater potential for liquid fuel production.[84,85] Among the bio-oils evaluated, this one also stood out for having the highest content of phenolic monomers, compounds of high commercial interest due to their potential as precursors in the production of high value-added chemicals.[67]

4. CONCLUSIONS

The pyrolysis of green coconut husks has demonstrated significant potential for valorizing this agro-industrial waste, enabling the production of biochars and bio-oils with properties that can be optimized by adjusting the processing temperature. The biochar obtained at 400 °C (46.9 wt.%) exhibited a more functionalized matrix, while the biochar produced at 600 °C (29.6 wt.%) showed greater aromatization and recalcitrance. Pyrolysis at 500 °C yielded a biochar with chemical properties intermediate between these two extremes, with a moderate yield (34.2 wt.%), a high degree of aromatization, and stability.

Regarding bio-oil, the products obtained at all three pyrolysis temperatures contained high levels of compounds of significant industrial and energy interest, including phenolic monomers and fatty acids. The highest bio-oil yield was achieved at 500 °C (11.0%), resulting in a product with a phenolic content of ∼50% by area, with the phenol monomer as the main molecule present. This offers a renewable alternative for industries that currently use petroleum-derived phenol. Additionally, the fatty acid content of ∼38% by area suggests promising potential for producing renewable hydrocarbons after further processing. The results indicate that pyrolysis at 500 °C simultaneously optimizes the quality of both liquid and solid products, making it an ideal condition for the energy and chemical utilization of green coconut biomass. Therefore, the pyrolysis of green coconut husks represents a sustainable and technically viable route for producing high value-added bioproducts.

■ ASSOCIATED CONTENT

Supporting Information

The Supporting Information is available free of charge at https://pubs.acs.org/doi/10.1021/acs.energyfuels.5c06504.

Schematic diagram of the pyrolysis reactor (Figure S1), proximal and elemental properties of biomass derived from green coconut husks (Table S1), composition of the gaseous product as a function of pyrolysis time (Figure S2), gravimetric yield of gaseous species produced by GCH pyrolysis (Table S2), TGA curves of bio-oils produced at different pyrolysis temperatures (Figure S3), comparison of chromatograms of bio-oils produced at 400, 500, and 600 °C (Figure S4), and compounds identified in GC/MS analyses of bio-oil samples from GCH biomass (Table S3) (PDF)

■ AUTHOR INFORMATION

Corresponding Author

Alberto Wisniewski, Jr. − *Petroleum and Energy from Biomass Research Group (PEB), Department of Chemistry, Federal University of Sergipe, São Cristóvão, SE 49107-230, Brazil;* orcid.org/0000-0001-6815-0265; Phone: +55 79 31947045; Email: albertowj@academico.ufs.br

Authors

Tarcísio Martins − *Petroleum and Energy from Biomass Research Group (PEB), Department of Chemistry, Federal University of Sergipe, São Cristóvão, SE 49107-230, Brazil;* orcid.org/0000-0003-1373-7987

Mirele Santana Sá − *Petroleum and Energy from Biomass Research Group (PEB), Department of Chemistry, Federal University of Sergipe, São Cristóvão, SE 49107-230, Brazil;* orcid.org/0000-0001-7283-7051

Miliana Gouveia Silva − *Petroleum and Energy from Biomass Research Group (PEB), Department of Chemistry, Federal University of Sergipe, São Cristóvão, SE 49107-230, Brazil*

Wenes Ramos da Silva − *Petroleum and Energy from Biomass Research Group (PEB), Department of Chemistry, Federal University of Sergipe, São Cristóvão, SE 49107-230, Brazil;* orcid.org/0000-0002-3485-2266

Complete contact information is available at: https://pubs.acs.org/10.1021/acs.energyfuels.5c06504

Funding

The Article Processing Charge for the publication of this research was funded by the Coordenacao de Aperfeicoamento de Pessoal de Nivel Superior (CAPES), Brazil (ROR identifier: 00x0ma614).

Notes

The authors declare no competing financial interest.

■ ACKNOWLEDGMENTS

The authors thank CAPES for the provision of a scholarship (88887.854541/2023-00) and CNPq for the financial support (303757/2024-8). The authors want to thank CLQM (Center of Multiusers Chemistry Laboratories) at the Federal University of Sergipe, the NEREES (Center for Renewable Energies and Energy Efficiency of Sergipe) at the Sergipe Technology Park (SergipeTec), and the Center for Studies in Colloidal Systems at the Institute of Technology and Research for the analytical assistance.

■ REFERENCES

(1) Wegelin, S.; Meier, M. A. R. Bio-Based Aromatics for Chemicals and Materials: Advances in Renewable Drop-in and Functional Alternatives. *Curr. Opin. Green Sustain. Chem.* **2024**, *47*, No. 100931.
(2) Wang, Y.; Liu, Z.; Deng, H.; Cao, P.; Tan, T.; Wang, D.; Liu, G. Study on the Properties and Components of Solid-Liquid Products by Co-Pyrolysis of Sludge and Cotton Stalk. *J. Anal. Appl. Pyrolysis* **2024**, *182*, No. 106712.
(3) Pawar, A.; Panwar, N. L.; Jain, S.; Jain, N. K.; Gupta, T. Thermal Degradation of Coconut Husk Waste Biomass under Non-Isothermal Condition. *Biomass Convers. Biorefinery* **2023**, *13* (9), 7613−7622.
(4) Food and Agriculture Organization Statistics *Crops and livestock products [database]*. https://www.fao.org/faostat/en/#data/QCL (accessed May 02, 2025).
(5) Instituto Brasileiro de Geografia e Estatística *Produção de Coco-da-baía*. https://www.ibge.gov.br/explica/producao-agropecuaria/coco-da-baia/br (accessed May 02, 2025).
(6) Grass Ramírez, J. F.; Muñoz, R. C.; Zartha Sossa, J. W. Innovations and Trends in the Coconut Agroindustry Supply Chain: A Technological Surveillance and Foresight Analysis. *Front. Sustainable Food Syst.* **2023**, *7*, 1048450.
(7) Nunes, L. A.; Silva, M. L. S.; Gerber, J. Z.; Kalid, R. de A. Waste Green Coconut Shells: Diagnosis of the Disposal and Applications for Use in Other Products. *J. Clean. Prod.* **2020**, *255*, No. 120169.
(8) Vieira, F.; Santana, H. E. P.; Jesus, M.; Santos, J.; Pires, P.; Vaz-Velho, M.; Silva, D. P.; Ruzene, D. S. Coconut Waste: Discovering Sustainable Approaches to Advance a Circular Economy. *Sustainability* **2024**, *16* (7), 3066.
(9) Agrizzi, T.; Oliveira, M. A.; Faria, E. V.; Santos, K. G.; Xavier, T. P.; Lira, T. S. Assessing Coconut Shell Pyrolysis: Biomass Characterization, Activation Energy Estimation, and Statistical Analysis of Operating Conditions. *Bioresour. Technol. Reports* **2024**, *26*, No. 101831.
(10) Bisen, D.; Chouhan, A. P. S.; Pant, M.; Chakma, S. Advancement of Thermochemical Conversion and the Potential of Biomasses for Production of Clean Energy: A Review. *Renew. Sustain. Energy Rev.* **2025**, *208*, No. 115016.
(11) Wei, F.; Sang, S.; Liu, S.; Zhao, J.-P.; Zhao, X.-Y.; Cao, J.-P. BECCS Carbon-Negative Technologies Based on Biomass Thermochemical Conversion: A Review of Critical Pathways and Research Advances. *Fuel* **2025**, *390*, No. 134743.
(12) Ungureanu, N.; Vlăduţ, N.-V.; Biriş, S.-Ş.; Gheorghiţă, N.-E.; Ionescu, M. Biomass Pyrolysis Pathways for Renewable Energy and Sustainable Resource Recovery: A Critical Review of Processes, Parameters, and Product Valorization. *Sustainability* **2025**, *17* (17), 7806.
(13) Guo, J.; Zhou, H.; Jia, L.; Wang, Y.; Fan, M. Effects of Biochar from Different Pyrolysis Temperatures on Soil Physical Properties and Hydraulic Characteristics in Potato Farmland of Arid and Semi-Arid Regions. *Agric. Water Manag.* **2025**, *313*, No. 109483.
(14) Tan, Y. C.; Jia, S.; Tan, J.; Leow, Y.; Zheng, R.; Tan, X. Y.; Dolmanan, S. B.; Zhang, M.; Yew, P. Y. M.; Ni, X. P.; Zhu, Q.; Xu, J.; Loh, X. J.; Ramakrishna, S.; Kai, D. Coconut Husk-Derived Biochar for Enhancing Electrochemical Conversion of CO2. *Mater. Today Chem.* **2023**, *30*, No. 101595.
(15) Peixoto, B. S.; de Oliveira Mota, L. S.; Dias, I. M.; Muzzi, B.; Albino, M.; Petrecca, M.; Innocenti, C.; de Oliveira, P. C. O.; Romeiro, G. A.; Sangregorio, C.; de Moraes, M. C. An Alternative Synthesis of Magnetic Biochar from Green Coconut Husks and Its Application for Simultaneous and Individual Removal of Caffeine and Salicylic Acid from Aqueous Solution. *J. Environ. Chem. Eng.* **2023**, *11* (5), No. 110835.
(16) Dissanayaka, D. M. N. S.; Udumann, S. S.; Nuwarapaksha, T. D.; Atapattu, A. J. Effects of Pyrolysis Temperature on Chemical Composition of Coconut-Husk Biochar for Agricultural Applications: A Characterization Study. *Technol. Agron.* **2023**, *3* (1), 13.
(17) Silva, W. R.; Santos, R. M.; Wisniewski, A. Continuous Rotary Kiln Pyrolysis of Cassava Plant Shoot System and Wide Speciation of Oxygenated and Nitrogen-Containing Compounds in Bio-Oil by HESI and APPI-Orbitrap MS. *Bioresour. Technol.* **2024**, *404*, No. 130915.
(18) Andrade, Y. B.; dos Santos Polidoro, A.; Schneider, J. K.; dos Santos Freitas, L.; Caramão, E. B.; de Oliveira Farrapeira, R. Influence of Residual Biomass Deposition Time of Green Coconut on the Quality of Bio-Oil Generated by Pyrolysis. *J. Anal. Appl. Pyrolysis* **2024**, *179*, No. 106436.
(19) Santos, D. M.; Cruz, A. S. A.; Andrade, Y. B.; dos Santos, P. N. A.; Schneider, J. K.; Caramão, E. B. Co-Pyrolysis of Green Coconut Fibers with Polymers: Enhanced the Quality of Produced Bio-Oil Aiming Bio-Fuel Production. *Biomass and Bioenergy* **2026**, *205*, No. 108542.
(20) Junior, I. J. T.; Alves, J. L. F.; Brusamarello, C. Z.; Di Domenico, M. Impact of Operational Parameters on the Yield of Biochar, Bio-Oil, and Pyrolytic Gas in Lignocellulosic Biomass Pyrolysis: A Systematic Review. *Bioresour. Technol. Reports* **2025**, *30*, No. 102155.
(21) Ramani, B.; Anjum, A.; Bramer, E.; Dierkes, W.; Blume, A.; Brem, G. A Comprehensive Study on the Effect of the Pyrolysis Temperature on the Products of the Flash Pyrolysis of Waste Tires. *J. Environ. Chem. Eng.* **2025**, *13* (2), No. 115468.
(22) Handiso, B.; Pääkkönen, T.; Wilson, B. P. Effect of Pyrolysis Temperature on the Physical and Chemical Characteristics of Pine Wood Biochar. *Waste Manag. Bull.* **2024**, *2* (4), 281−287.
(23) Rambhatla, N.; Panicker, T. F.; Mishra, R. K.; Manjeshwar, S. K.; Sharma, A. Biomass Pyrolysis for Biochar Production: Study of Kinetics Parameters and Effect of Temperature on Biochar Yield and Its Physicochemical Properties. *Results Eng.* **2025**, *25*, No. 103679.
(24) Modak, S.; Katiyar, P.; Talukdar, D.; Gole, B. Pyrolytic Evaluation of Essential Oil Industry Waste: Effect of Pyrolysis Temperature on Bio-Oil Composition. *J. Environ. Manage.* **2025**, *392*, No. 126757.
(25) Pandiselvam, R.; Shaji, A.; Ramesh, S. V.; Sathyan, N.; Manikantan, M. R.; Mathew, A. C. Development, Evaluation, and Optimization of Portable Pyrolysis System for the Production of Biochar from Tender Coconut Husk. *Biomass Convers. Biorefinery* **2024**, *14* (16), 19285−19294.
(26) Gongxiang, S.; Yankui, W.; Dexin, H.; Hanjian, L.; Abdullahi, S. A.; Jun, X.; Long, J.; Yi, W.; Sheng, S.; Song, H.; Jun, X. The Heating Rate and Final Temperature Impacts on the Coconut Shell Char Structure Characteristics during Photo-Thermal Pyrolysis. *J. Anal. Appl. Pyrolysis* **2022**, *167*, No. 105695.
(27) Dhar, S. A.; Sakib, T. U.; Hilary, L. N. Effects of Pyrolysis Temperature on Production and Physicochemical Characterization of Biochar Derived from Coconut Fiber Biomass through Slow Pyrolysis Process. *Biomass Convers. Biorefinery* **2022**, *12* (7), 2631−2647.
(28) Huang, Y.-F.; Lo, S.-L. Predicting Heating Value of Lignocellulosic Biomass Based on Elemental Analysis. *Energy* **2020**, *191*, No. 116501.
(29) Melo, J. A.; Silva, L. A. de A.; Santos, J. M.; Wisniewski, A. Advanced Characterization of Oxidized Derivatives in Alternative Fatty Esters Mixture for Biodiesel Purposes. *Fuel* **2022**, *309*, No. 122109.
(30) Moura, H. O. M. A.; Câmara, A. B. F.; Campos, L. M. A.; de Carvalho, L. S. Novel Methodology for Lignocellulose Composition,

https://doi.org/10.1021/acs.energyfuels.5c06504
Energy Fuels XXXX, XXX, XXX−XXX

Polymorphism and Crystallinity Analysis Via Deconvolution of Differential Thermogravimetry Data. *J. Polym. Environ.* **2023**, *31* (5), 1915−1924.
(31) Stankovikj, F.; McDonald, A. G.; Helms, G. L.; Garcia-Perez, M. Quantification of Bio-Oil Functional Groups and Evidences of the Presence of Pyrolytic Humins. *Energy Fuels* **2016**, *30* (8), 6505−6524.
(32) Gonçalves, C.; Rodriguez-Jasso, R. M.; Gomes, N.; Teixeira, J. A.; Belo, I. Adaptation of Dinitrosalicylic Acid Method to Microtiter Plates. *Anal. Methods* **2010**, *2* (12), 2046.
(33) Nolte, M. W.; Liberatore, M. W. Viscosity of Biomass Pyrolysis Oils from Various Feedstocks. *Energy Fuels* **2010**, *24* (12), 6601−6608.
(34) Fonseca, F. G.; Funke, A.; Niebel, A.; Soares Dias, A. P.; Dahmen, N. Moisture Content as a Design and Operational Parameter for Fast Pyrolysis. *J. Anal. Appl. Pyrolysis* **2019**, *139*, 73−86.
(35) Puri, L.; Hu, Y.; Naterer, G. Critical Review of the Role of Ash Content and Composition in Biomass Pyrolysis. *Front. Fuels* **2024**, *2*, 1378361.
(36) Fatmawati, A.; Nurtono, T.; Widjaja, A. Thermogravimetric Kinetic-Based Computation of Raw and Pretreated Coconut Husk Powder Lignocellulosic Composition. *Bioresour. Technol. Reports* **2023**, *22*, No. 101500.
(37) Chen, D.; Cen, K.; Zhuang, X.; Gan, Z.; Zhou, J.; Zhang, Y.; Zhang, H. Insight into Biomass Pyrolysis Mechanism Based on Cellulose, Hemicellulose, and Lignin: Evolution of Volatiles and Kinetics, Elucidation of Reaction Pathways, and Characterization of Gas. *Biochar and Bio-oil. Combust. Flame* **2022**, *242*, No. 112142.
(38) Xu, J.; Jiang, J.; Zhao, J. Thermochemical Conversion of Triglycerides for Production of Drop-in Liquid Fuels. *Renew. Sustain. Energy Rev.* **2016**, *58*, 331−340.
(39) Ohra-aho, T.; Ghalibaf, M.; Alén, R.; Lindfors, C.; Oasmaa, A. Analysis of Lipophilic Extractives from Fast Pyrolysis Bio-Oils. *Energy Fuels* **2022**, *36* (11), 5797−5804.
(40) Nascimento, D. M. do; Almeida, J. S.; Vale, M. do S.; Leitão, R. C.; Muniz, C. R.; Figueirêdo, M. C. B. de; Morais, J. P. S.; Rosa, M. de F. A Comprehensive Approach for Obtaining Cellulose Nanocrystal from Coconut Fiber. Part I: Proposition of Technological Pathways. *Ind. Crops Prod.* **2016**, *93*, 66−75.
(41) Araújo Padilha, C. E. de; Costa Nogueira, C. da; Deus Junior, J. O. de; Cavalcante, J. D. N.; Costa de Araújo, B. M.; Alles de Jesus, A.; Braga, R. M.; Santana Souza, D. F. de. Simultaneous Saccharification and Fermentation Residues as Potential Sources of Phenolics by Fast Pyrolysis (Py-GC/MS) and Alkaline Hydrolysis. *Ind. Crops Prod.* **2024**, *208*, No. 117855.
(42) de Araújo, B. M. C.; Nunes, J. S.; da Costa Filho, J. D. B.; de Santana Souza, D. F.; de Araújo Padilha, C. E.; dos Santos, E. S. Adding-Value to Green Coconut Fiber by Producing Lignosulfonate for Enhancing the Sugar Release in Enzymatic Hydrolysis. *Waste and Biomass Valorization* **2025**, *16* (10), 5561−5572.
(43) Chen, N.; Pilla, S. A Comprehensive Review on Transforming Lignocellulosic Materials into Biocarbon and Its Utilization for Composites Applications. *Compos. Part C Open Access* **2022**, *7*, No. 100225.
(44) Kim, H.; Yu, S.; Kim, M.; Ryu, C. Progressive Deconvolution of Biomass Thermogram to Derive Lignocellulosic Composition and Pyrolysis Kinetics for Parallel Reaction Model. *Energy* **2022**, *254*, No. 124446.
(45) Zhang, Y.; Liang, Y.; Li, S.; Yuan, Y.; Zhang, D.; Wu, Y.; Xie, H.; Brindhadevi, K.; Pugazhendhi, A.; Xia, C. A Review of Biomass Pyrolysis Gas: Forming Mechanisms, Influencing Parameters, and Product Application Upgrades. *Fuel* **2023**, *347*, No. 128461.
(46) Vilas-Boas, A. C. M.; Tarelho, L. A. C.; Moura, J. M. O.; Gomes, H. G. M. F.; Marques, C. C.; Pio, D. T.; Nunes, M. I. S.; Silvestre, A. J. D. Methodologies for Bio-Oil Characterization from Biomass Pyrolysis: A Review Focused on GC-MS. *J. Anal. Appl. Pyrolysis* **2025**, *185*, No. 106850.
(47) del Carmen Recio-Ruiz, M.; Ruiz-Rosas, R.; García-Mateos, F. J.; Valero-Romero, M. J.; Rosas, J. M.; Rodríguez-Mirasol, J.; Cordero, T. An Integrated Approach to the Valorization of Pyrolysis Products from Lignocellulosic Residues and By-Products. *Biomass Bioenergy* **2025**, *196*, No. 107676.
(48) Bridgwater, A. V. Review of Fast Pyrolysis of Biomass and Product Upgrading. *Biomass and Bioenergy* **2012**, *38*, 68−94.
(49) Carregosa, I. S. C.; Carregosa, J. de C.; Silva, W. R.; Santos, T. M.; Wisniewski, A., Jr Thermochemical Conversion of Aquatic Weed Biomass in a Rotary Kiln Reactor for Production of Bio-Based Derivatives. *J. Anal. Appl. Pyrolysis* **2023**, *173*, No. 106048.
(50) Li, Y.; Gupta, R.; Zhang, Q.; You, S. Review of Biochar Production via Crop Residue Pyrolysis: Development and Perspectives. *Bioresour. Technol.* **2023**, *369*, No. 128423.
(51) Tomczyk, A.; Sokołowska, Z.; Boguta, P. Biochar Physicochemical Properties: Pyrolysis Temperature and Feedstock Kind Effects. *Rev. Environ. Sci. Bio/Technology* **2020**, *19* (1), 191−215.
(52) Balmuk, G.; Videgain, M.; Manyà, J. J.; Duman, G.; Yanik, J. Effects of Pyrolysis Temperature and Pressure on Agronomic Properties of Biochar. *J. Anal. Appl. Pyrolysis* **2023**, *169*, No. 105858.
(53) Silva, W. R.; Santos, R. M.; Wisniewski, A., Jr Cassava's Harvest Residue Biochar from Rotary Kiln Pyrolysis: Effects on Sandy Loam Soil Properties and Maize Growth. *Biomass and Bioenergy* **2026**, *205*, No. 108464.
(54) Zhang, H.; Wang, T.; Sui, Z.; Zhang, Y.; Sun, B.; Pan, W.-P. Enhanced Mercury Removal by Transplanting Sulfur-Containing Functional Groups to Biochar through Plasma. *Fuel* **2019**, *253*, 703−712.
(55) Tan, L.; Ma, Z.; Yang, K.; Cui, Q.; Wang, K.; Wang, T.; Wu, G.-L.; Zheng, J. Effect of Three Artificial Aging Techniques on Physicochemical Properties and Pb Adsorption Capacities of Different Biochars. *Sci. Total Environ.* **2020**, *699*, No. 134223.
(56) Wang, C.; Xia, S.; Cui, C.; Kang, S.; Zheng, A.; Yu, Z.; Zhao, Z. Investigation into the Correlation between the Chemical Structure of Lignin and Its Temperature-Dependent Pyrolytic Product Evolution. *Fuel* **2022**, *329*, No. 125215.
(57) Vuppaladadiyam, A. K.; Varsha Vuppaladadiyam, S. S.; Sikarwar, V. S.; Ahmad, E.; Pant, K. K.; S, M.; Pandey, A.; Bhattacharya, S.; Sarmah, A.; Leu, S.-Y. A Critical Review on Biomass Pyrolysis: Reaction Mechanisms, Process Modeling and Potential Challenges. *J. Energy Inst.* **2023**, *108*, No. 101236.
(58) Shah, M. A.; Khan, N. S.; Kumar, V.; Qurashi, A. Pyrolysis of Walnut Shell Residues in a Fixed Bed Reactor: Effects of Process Parameters, Chemical and Functional Properties of Bio-Oil. *J. Environ. Chem. Eng.* **2021**, *9* (4), No. 105564.
(59) Zheng, K.; Hu, S.; Gong, Z.; Jia, M.; Xu, K.; Xu, J.; Jiang, L.; Wang, Y.; Su, S.; Xiang, J. Interaction among Cellulose, Hemicellulose and Lignin during Pressurized Pyrolysis: Importance of Deoxygenation and Aromatization Reactions. *Energy* **2025**, *314*, No. 134320.
(60) Ma, Z.; Yang, Y.; Wu, Y.; Xu, J.; Peng, H.; Liu, X.; Zhang, W.; Wang, S. In-Depth Comparison of the Physicochemical Characteristics of Bio-Char Derived from Biomass Pseudo Components: Hemicellulose, Cellulose, and Lignin. *J. Anal. Appl. Pyrolysis* **2019**, *140*, 195−204.
(61) Esteves, B.; Sen, U.; Pereira, H. Influence of Chemical Composition on Heating Value of Biomass: A Review and Bibliometric Analysis. *Energies* **2023**, *16* (10), 4226.
(62) Melo, J. A.; de Sá, M. S.; Moral, A.; Bimbela, F.; Gandía, L. M.; Wisniewski, A. Renewable Hydrocarbon Production from Waste Cottonseed Oil Pyrolysis and Catalytic Upgrading of Vapors with Mo-Co and Mo-Ni Catalysts Supported on γ-Al2O3. *Nanomaterials* **2021**, *11* (7), 1659.
(63) Sun, K.; Guo, T.; Li, Y.; Wang, W.; Li, Z.; Geng, P.; Fu, P. Rapid Pyrolysis of Cellulose: Revealing the Role of Volatile Matter and Char Structure Evolution. *J. Anal. Appl. Pyrolysis* **2024**, *182*, No. 106704.
(64) Zhong, Y.; Gao, W.; Li, C.; Ding, Y. Pyrolysis Mechanism Study on Xylose by Combining Experiments, Chemical Reaction Neural Networks and Density Functional Theory. *Bioresour. Technol.* **2025**, *429*, No. 132530.
(65) Miro de Medeiros, A.; de Sousa Castro, K.; Gundim de Macêdo, M. L.; de Morais Araújo, A. M.; Ribeiro da Silva, D.;

https://doi.org/10.1021/acs.energyfuels.5c06504
Energy Fuels XXXX, XXX, XXX−XXX

Gondim, A. D. Catalytic Pyrolysis of Coconut Oil with Ni/SBA-15 for the Production of Bio Jet Fuel. *RSC Adv.* **2022**, *12* (16), 10163−10176.
(66) Qiu, Y.; Zhong, D.; Zeng, K.; Li, J.; Flamant, G.; Nzihou, A.; Yang, H.; Chen, H. Effects of Cellulose-Lignin Interaction on the Evolution of Biomass Pyrolysis Bio-Oil Heavy Components. *Fuel* **2022**, *323*, No. 124413.
(67) Fonts, I.; Lázaro, C.; Cornejo, A.; Sánchez, J. L.; Afailal, Z.; Gil-Lalaguna, N.; Arauzo, J. M. Bio-Oil Fractionation According to Polarity and Molecular Size: Characterization and Application as Antioxidants. *Energy Fuels* **2024**, *38* (19), 18688−18704.
(68) Li, Z.; Shi, L.; Liang, D.; Li, F.; Wei, L.; Li, W.; Zha, X. Study on the Hydrocarbon-Rich Bio-Oil from Catalytic Fast Co-Pyrolysis Cotton Stalk and Polypropylene over Alkali-Modified HZSM-5. *Ind. Crops Prod.* **2025**, *224*, No. 120352.
(69) Silva, R. S.; da Silva, R. A.; de Andrade, F. M.; Acácio Neto, P. N.; do Nascimento, R. M.; Santos, J. M.; Stragevitch, L.; Pimentel, M. F.; Simoes, D. A.; Danielski, L. Hydrothermal Liquefaction of Sugarcane Bagasse and Straw: Effect of Operational Conditions on Product Fractionation and Bio-Oil Composition. *Energies* **2024**, *17* (21), 5439.
(70) Araujo, L. M.; Santos, M. A.; Brandão, S. T.; Lima, S. B.; Pires, C. A. M. Study of the Pectin Influence on Bio-Oil Produced from Sisal Residue Pyrolysis. *J. Anal. Appl. Pyrolysis* **2023**, *170*, No. 105906.
(71) Yang, T.; Liu, X.; Li, R.; Li, B.; Kai, X. Hydrothermal Liquefaction of Sewage Sludge to Produce Bio-Oil: Effect of Co-Pretreatment with Subcritical Water and Mixed Surfactants. *J. Supercrit. Fluids* **2019**, *144*, 28−38.
(72) Tian, Y.; Wang, F.; Djandja, J. O.; Zhang, S.-L.; Xu, Y.-P.; Duan, P.-G. Hydrothermal Liquefaction of Crop Straws: Effect of Feedstock Composition. *Fuel* **2020**, *265*, No. 116946.
(73) ZHANG, Y.; CHEN, D.; ZHANG, D.; ZHU, X. TG-FTIR Analysis of Bio-Oil and Its Pyrolysis/Gasification Property. *J. Fuel Chem. Technol.* **2012**, *40* (10), 1194−1199.
(74) Xu, H.; Li, J.; Zhong, D.; Zeng, K.; Zuo, H.; Zhang, X.; Vladimirovich, V. S.; Yang, H.; Chen, H. The Effect of Coke and Soot Formation on the Bio-Oil Combustion at High Temperatures. *J. Energy Inst.* **2023**, *111*, No. 101386.
(75) Santos, J.; Ouadi, M.; Jahangiri, H.; Hornung, A. Valorisation of Lignocellulosic Biomass Investigating Different Pyrolysis Temperatures. *J. Energy Inst.* **2020**, *93* (5), 1960−1969.
(76) Cai, J.; Banks, S. W.; Yang, Y.; Darbar, S.; Bridgwater, T. Viscosity of Aged Bio-Oils from Fast Pyrolysis of Beech Wood and Miscanthus: Shear Rate and Temperature Dependence. *Energy Fuels* **2016**, *30* (6), 4999−5004.
(77) Oginni, O.; Singh Tingi, K. Temperature-dependent Viscosity of Bio-oil Derived from White Pine and Norway Spruce Needles. *Biofuels, Bioprod. Biorefining* **2021**, *15* (5), 1520−1525.
(78) Kwon, D.; Kim, Y.; Choi, D.; Jung, S.; Tsang, Y. F.; Kwon, E. E. Enhanced Thermochemical Valorization of Coconut Husk through Carbon Dioxide Integration: A Sustainable Approach to Agricultural Residue Utilization. *Appl. Energy* **2024**, *369*, No. 123576.
(79) Yu, J.; Wang, D.; Sun, L. The Pyrolysis of Lignin: Pathway and Interaction Studies. *Fuel* **2021**, *290*, No. 120078.
(80) Wang, L.; Yi, W.; Zhang, A.; Li, Z.; Cai, H.; Li, Y. Catalytic Fast Pyrolysis of Corn Stalk for Phenols Production With Solid Catalysts. *Front. Energy Res.* **2019**, *7*, 86.
(81) Dudnikova, T.; Wong, M. H.; Minkina, T.; Sushkova, S.; Bauer, T.; Khroniuk, O.; Barbashev, A.; Shuvaev, E.; Nemtseva, A.; Kravchenko, E. Effects of Pyrolysis Conditions on Sewage Sludge-Biochar Properties and Potential Risks Based on PAH Contents. *Environ. Res.* **2025**, *266*, No. 120444.
(82) Kim, Y.-M.; Jae, J.; Myung, S.; Sung, B. H.; Dong, J.-I.; Park, Y.-K. Investigation into the Lignin Decomposition Mechanism by Analysis of the Pyrolysis Product of Pinus Radiata. *Bioresour. Technol.* **2016**, *219*, 371−377.
(83) Leng, L.; Zheng, H.; Shen, T.; Wu, Z.; Xiong, T.; Liu, S.; Cao, J.; Peng, H.; Zhan, H.; Li, H. Engineering Biochar from Biomass Pyrolysis for Effective Adsorption of Heavy Metal: An Innovative Machine Learning Approach. *Sep. Purif. Technol.* **2025**, *361*, No. 131592.
(84) Gollakota, A. R. K.; Shu, C.-M.; Sarangi, P. K.; Shadangi, K. P.; Rakshit, S.; Kennedy, J. F.; Gupta, V. K.; Sharma, M. Catalytic Hydrodeoxygenation of Bio-Oil and Model Compounds - Choice of Catalysts, and Mechanisms. *Renew. Sustain. Energy Rev.* **2023**, *187*, No. 113700.
(85) Santos, B. S. D. F.; Palacios-Bereche, M. C.; Gallego, A. G.; Nebra, S. A.; Palacios-Bereche, R. Energy Assessment and Heat Integration of Biofuel Production from Bio-Oil Produced through Fast Pyrolysis of Sugarcane Straw, and Its Upgrading via Hydrotreatment. *Renew. Energy* **2024**, *232*, No. 121021.

https://doi.org/10.1021/acs.energyfuels.5c06504
Energy Fuels XXXX, XXX, XXX−XXX